TECHNISCHE UNIVERSITÄT WIEN
Vienna University of Technology

MASTERARBEIT

Performance assessment and modeling of a brick made 'Sonnenhaus' in Zwettl.

unter der Leitung von

Univ.-Prof. Dipl.-Ing. Dr.techn. Ardeshir Mahdavi

E 259-3 Abteilung für Bauphysik und Bauökologie

Institut für Architekturwisenschaften

eingereicht an der

Technischen Universität Wien

Fakultät für Architektur und Raumplanung

von

Aleksandra Piewald

1227974.

Marchettigasse 7/11, 1060 Wien

Wien, September 2014

Abstract

In this Master's thesis the performance of a heat delivery system of an energy efficient single-family house located in Zwettl, Lower Austria, is investigated. Over the course of ten months, in which the building was inhabited, monitoring data of the heat delivered to the floor and brick walls was collected. Using these data, a detailed analysis of the building's performance is presented. In particular, it is compared to the simulation model that was created during the design phase of the house. It turns out that the design phase model is rather inaccurate and often does not match the actual behavior.

Consequently, this simulation model is investigated and enhanced. Particular improvements concern the following input parameters of the building regime: set temperature points, natural ventilation, infiltration, internal heat gains and weather data. Most of these are based on the actual user behavior, which was derived from additional sensors in the building (e.g. temperature, CO2 concentration, etc.).

The results are presented by comparing the improved simulation to the design phase model and to the actual monitoring data in a monthly evaluation. The particular influence of each mentioned parameter is analyzed and discussed separately. It is shown that the enhanced simulation much more accurately models the reality.

Keywords

thermal simulation, monitoring, solar energy, model calibration, heating demand

Contents

Acknowledgments

I would like to express my gratitude to Professor Dr. Ardeshir Mahdavi for his commitment and guidance during supervision of the thesis. Further, to Matthias Schuß for his constant patience and support. I would like to express my deep gratitude to Energy Department in Austrian Institute of Technology, especially to Tim Selke for giving me possibility to work on the thesis and for his continuous assistance. I also want to thank ZAMG (Zentralanstalt für Meteorologie und Geodynamik) for providing me access to the weather data. Furthermore I am thankful to my family and closest friends who are always there for me. Above all I would like to thank my beloved husband for his support throughout my entire studies.

1 INTRODUCTION

1.1 Overview

The concept of a plus energy house is to deliver more energy in annual balance than it consumes. Renewable energy sources, such as wind power, hydropower, solar energy, biomass, biofuel or geothermal energy must be used for the production. The idea does not focus on the energy demand for heating alone, but has a holistic view of the overall energy performance of the building, including energy balances for heating, cooling, domestic hot water preparation and electricity. This goal is achieved using a combination of microgeneration technology (small-scale generation of heat and electric power) and low-energy building techniques such as passive solar building design, careful site selection and placement and good insulation (Disch 2009).

This thesis investigates an already constructed plus energy residential house in Zwettl, Lower Austria. In the following, this building will be referred to as *Sonnenhaus*. The remaining sections of this chapter give history and background information about the building.

Chapter 2, *Method*, briefly describes the main ideas and hypotheses of the work. Also, the used simulation and calculation tools are listed.

In order to effectively assess the energy efficiency of a building, it is crucial to install a monitoring system for all energy consumers and producers in the building. The particular monitoring system of the *Sonnenhaus* is described in detail in Chapter 3, *Performance Evaluation*.

In Chapter 4, *Creation of the Building Model*, the user-independent parameters of the simulation are described. These encompass the building envelope (construction, materials) and the weather data.

As the main part of the thesis, the original simulation model is improved step by step, adding complexity and additional information. The particular steps and methods are explained in Chapter 5, *Definition of the Building Regime*.

Finally, Chapter 6, *Results and Analysis*, presents the simulation results of the improved model and compares them to the recorded values of the monitoring system as well as to the original model from the design phase. Furthermore, the influence of each particular parameter is shown and discussed.

An overall conclusion, summing up the benefits to the improved model is given in Chapter 7, Conclusion.

1.2 Background

A *Sonnenhaus* building concept for a brick constructed dwelling was developed within the Austrian research project "Solar Plus Haus". The initiator of the project was Wienerberger AG. The Austrian Institute of Technology (AIT) did scientific support in the planning which was implemented in the "e4 Ziegelhaus 2020", a one-family house located in Zwettl in Lower Austria.

The construction of the building was finished during the first half of the year 2012. The building envelope is realized by a new technology of energy efficient bricks of Wienerberger AG.

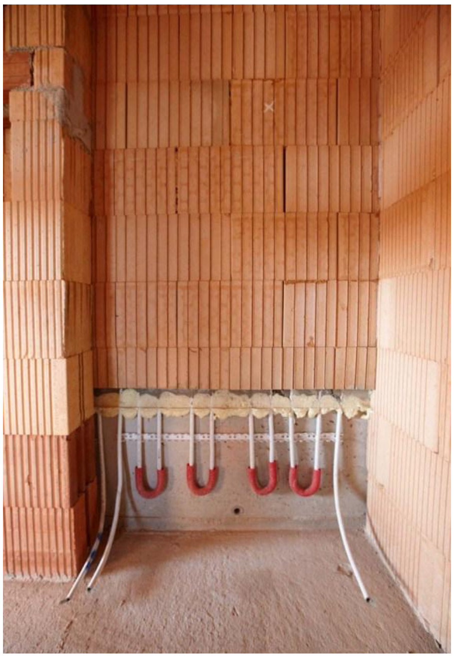

Figure 1: Thermally activated brick wall heating system.
(Source: AIT Austrian Institute of Technology GmbH, 2012)

Figure 2: Porotherm 44 W- The brick with included thermal insulation.
(Source: AIT Austrian Institute of Technology GmbH, 2012)

The architecture and energetic building concept is based on high energy efficiency in the building envelope. Solar technologies are used to cover the heat and electricity needs of the building operation, including user related energy demand. Around 50 m² flat- plate collectors are placed on a roof with a slope of 60° south orientation. This solar thermal system covers the hot water and heat requirements of the building. Especially designed water tank with a volume of 9,580 liters is situated within the thermal envelope over two floors. During the sunless winter days, when solar heat is not sufficient, a 40 kW wood boiler provides heat. In order to heat the rooms in winter, the hot water from the tank is mechanically circulated in the conventional floor heating in the living room and in numerous thermally activated brick walls. In addition, a photovoltaic system with 35 modules and a power peak of 6.5 kW is mounted on the garage roof and provides about the amount of electricity to fulfill the total annual electricity consumption of the building operation including users' needs. The solar power that is being delivered by the photovoltaic system might be used directly for the householders needs or might be fed into the public grid (Joechl 2013).

Figure 3: Photo of the main building.
(Source: Wienerberger Ziegelindustrie GmbH, 2013)

In the picture below the cross section of the building with relevant elements of the energy system is presented. The important elements are:

1. Building envelope with high thermal insulation
2. Thermally activated brick walls
3. Solar thermal collectors
4. Hot water tank as thermal storage
5. Biomass boiler

Figure 4: Cross section of the building.
(Source: Selke et al. 2012)

The AIT assesses the energy performance of the building by means of scientific monitoring since autumn 2012. This monitoring phase is planned until the mid of 2014. Due to the fact that preliminary calculation that have been performed by the AIT, resulted in a negative annual primary energy balance for the non-renewable part of energy the building is classified as a plus energy building.

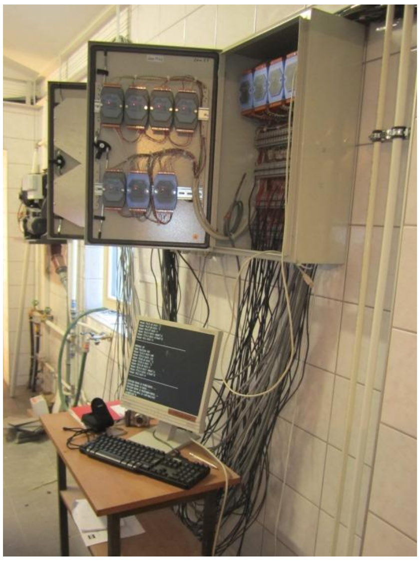

Figure 5: Monitoring system in technical room.
(Source: AIT Austrian Institute of Technology GmbH; 2012)

1.3 Research Methodology

The master thesis presents the heating energy target of the planning phase and the heating energy performance measured during the operational phase. It shows the energy performance of the brick made residential building from January until October 2013 and compares the measured data with the expected behavior. Furthermore, the thermal comfort in the building is examined. The main target of the thesis is to develop a numerical simulation model of the building, which meets the actual building performance.

The monitoring system in the building is in operation since October 2012. The observation time range for this thesis started on 1st of January 2013 and ended on 31th of October 2013.

This time range comprises all vital periods for an evaluation of the thermal energy. It contains the heating season, the season with rising sun activity, rising ambient temperature and the hot weather conditions of the summer.

In intervals of 5 minutes, a total of 183 individual data points are recorded. The values that are measured and used for the simulations and analysis are:

- ambient temperature
- temperature of the air in selected rooms
- ambient and indoor relative humidity
- CO_2 concentration in the rooms
- electric current consumed
- solar heat delivered
- biomass heat delivered
- wall heating delivered to the brick walls
- floor heating system
- domestic hot water

Due to the vast amount of data it is possible to generate detailed monthly analyses of energy balance of the building based on 10 month performance. After the proper filtering of the data, the heating energy balance based on actual building performance is presented. In the second step the aim is to develop and implement a new building model in the simulation environment based on the monitored data in order to compare the thermal simulation results of the building in TRNSYS17 with the measured building performance. This is planned to be done by defining proper algorithms in Matlab, based on available data from the monitoring phase, in order to create schedules defining all parameters that are necessary for the simulations as we all and its verification. The last step is to check the correct implementation of the model and the correct representation of the input parameters and logical structure of the model.

The following steps represent the method that has been applied.

- Plausibility Evaluation of the Monitoring Data
- Data Preparation for the Analyses
- Calculation of the Modeling Scenario
- Assessment of the Results

1.4 Motivation

The main goal of this Master Thesis is to verify how close the results of the thermal simulation are to the measured building performance. The accuracy of analysis software is important, but in the case of a thermal analysis tool this is not a simple question to answer. The main purpose for simulation is to model as close as possible a real-world physical process. To be useful it is important that simulation results closely match those from physical measurements taken in a similar actual situation. In our study case not all data, that should be used as an input parameters were being recorded. Therefore we generate the proper input parameters for the simulation, defining the actual physical processes, based on different than requested information from the monitoring.

In addition to this it is also important to first ensure that what is being calculated and what is being measured are actually comparable. Therefore the energy heating demands from the monitoring will be compared with the simulation results after the proper evaluation of the monitoring data. Moreover the possible reasons of differences appearing in the thermal building simulation results correspond with the actual building performance will be presented.

2 METHOD

2.1 Overview

The definition of the building construction and materials in the simulation rests upon existing documentation of the object. All assumptions that were based on statistical data are subsequently substituted by observed conditions. Specific weather situations and user behavior is also taken into account. The thermal simulation results and the comparison with the monitoring allow assessing the accuracy of the model.

2.2 Hypothesis

It is assumed that the thermal simulation results, after defining all input parameters based on actual monitored data, reflect the measured building performance (heat delivered into the wall and brick heating). Therefore the goal of this thesis is to calibrate the simulation with the values obtained by monitoring the existing *Sonnenhaus* in Zwettl. Measured data allows the simulation results to be confirmed and made more accurate. The detailed studies of the individual factors shall provide a reference for further research on the sensitivity of thermal simulations.

2.3 Selection of the Simulation Tool

In order to perform a dynamic thermal simulation of the building, it was decided to use TRNSYS17, a transient systems simulation program with a modular structure. It recognizes a system description language in which the user specifies the components that constitute the system and the manner in which they are connected. The TRNSYS library includes many of the components commonly found in thermal and electrical energy systems, as well as component routines to handle the input of weather data or other time-dependent forcing functions. TRNSYS is well suited for detailed analysis of any building system whose behavior is time dependent. (Duffy 2013). Due to the complexity of a multizone building, the model is not defined directly in the TRNSYS input file. Instead, a so-called *building file* (*.BUI) containing the required information is applied. In order to provide an easy-to-use visual interface for creating the BUI file we used the TRNBUILD tool.

The simulation was created in the following steps:

- Design of a 3D model of the existing building in Google SketchUp with the TRNSYS3D plugin.
- Assigning the relevant information about the building to the model in TRNBUILD.
- Introducing the weather file provided by ZAMG.
- Generation of the input parameters, defining the regime of the building, based on monitored conditions.
- Simulation of the system in hourly measurement steps, with defined introduced input parameters.

3 PERFORMANCE EVALUATION

3.1 Data Evaluation and Analysis

The building is equipped with sensor devices for room climate, outdoor climate, energy fluxes and various temperatures of the thermal system. Every sensor device provides a certain physical value to the monitoring system. The recorded data are collected by a computer system located inside the building (internal data processing) and then continuously transmitted via the Internet to a database server, which stores the complete set of data. For analysis, the data are downloaded on demand and combined with meta-data (e.g. physical unit, data node name, conversion factors, offsets). This is done by Matlab procedures which generate Matlab archive files (one per month). The data in the archive files are then available for analysis and graphical representations like diagrams and tables. The data path of the monitoring system is presented in *Figure 6*.

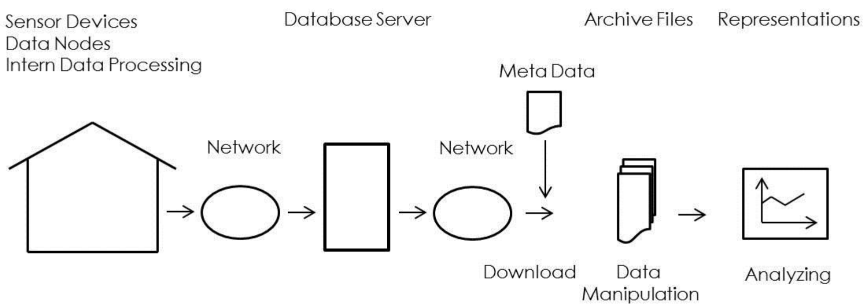

Figure 6: Data path of the monitoring system.
(Source: Joechl, 2013)

The first step to ensure the functionality of the monitoring system and the recorded data was a verification and quality control of the collected measurements. The data of the sensors were documented by defining their position, the function and the physical unit. With the help of statistic methods (extreme values, mean, median, standard deviation) it was possible to detect and filter obvious errors in the data. Moreover it was necessary to carry out an individual verification for certain data points to precisely identify existing gaps in the data records. Such individual assessments and corrections were necessary for the temperature sensors, relative humidity (Rh) and CO2 concentration in the monitored rooms.

TRNSYS17 requires input data in hourly intervals. Therefore, the monitoring data, which is available in 5 minutes intervals had to be averaged over 60 minutes.

In the collected data set we could observe three major gaps, in March 2013 for 83 h, in April 2013 for 222 h and in July 2013 for 100 h. Additionally, the electric demand sensors did not deliver any data for all of January, February and October. The gaps occurred due to downtimes of the recording servers.

Sensor group	1.01. - 28.02	28.03. – 31.03	26.04. – 1.05	4.07 - 8.07	1.10.- 31.10
Indoor climate		x	x	x	
Electrical demand	x	x	x	x	x
Indoor CO2 level		x	x	x	

Table 1*: Visualization of gaps in data sets for particular sensor groups.*

Figure 7 and *Figure 8* show the sensor positions on the floor plan of the building.

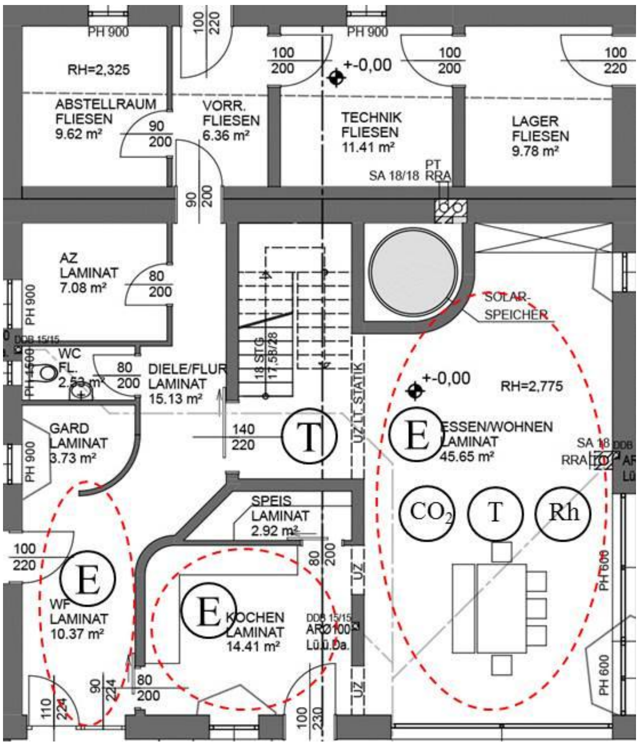

Figure 7: First floor plan and the sensors positions.
(Source: Franz Schiller GmbH, 2012)

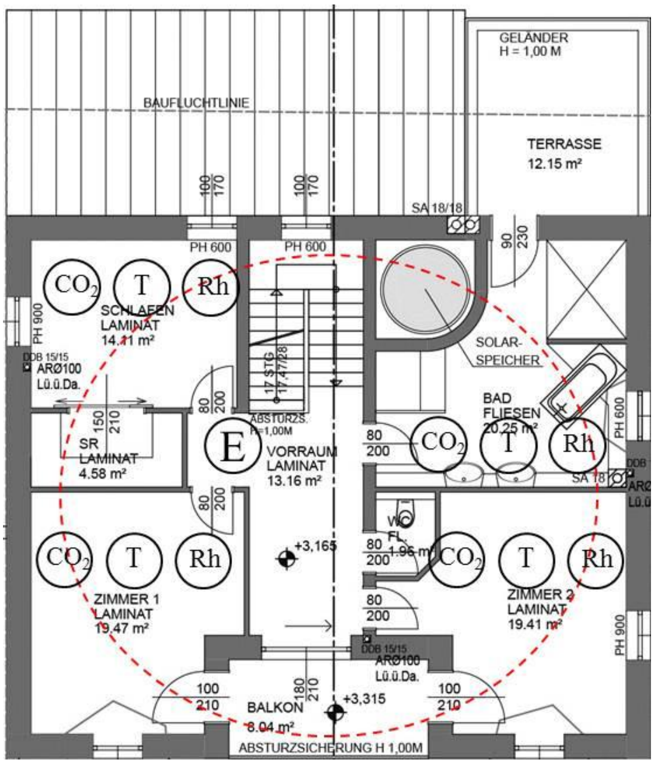

Figure 8: Second floor plan and the sensors positions
(Source: Franz Schiller GmbH, 2012)

Three types of sensors were used to record the data:

- Combined sensor for CO_2, temperature and relative humidity
- Electric energy meter
- Temperature sensor

The specifications and descriptions are presented in the appendix.

3.2 Heating Energy Balance

For a deeper understanding of the energy system, the major energy balances and fluxes are introduced. These energy contributions are also the input for the comparison with the modeling in the next sections.

The *Figure 9* presents the energy balances for heat. It shows the quantities for every month in the observed time range. *Table 2* shows the numerical values of the energy balances for heat in 10 months.

Each applied time period, which was adapted to the available monitoring data lasted for exactly one month, from the first day of each month (24:00), until the first day of the following month with one exception- April and May. In the months mentioned above due to a data gap, the applied time period was lasting one day longer in April- until the second of May, and respectively one day shorter in May. A table with applied time periods, which are adapted to the available monitoring data is available in the appendix.

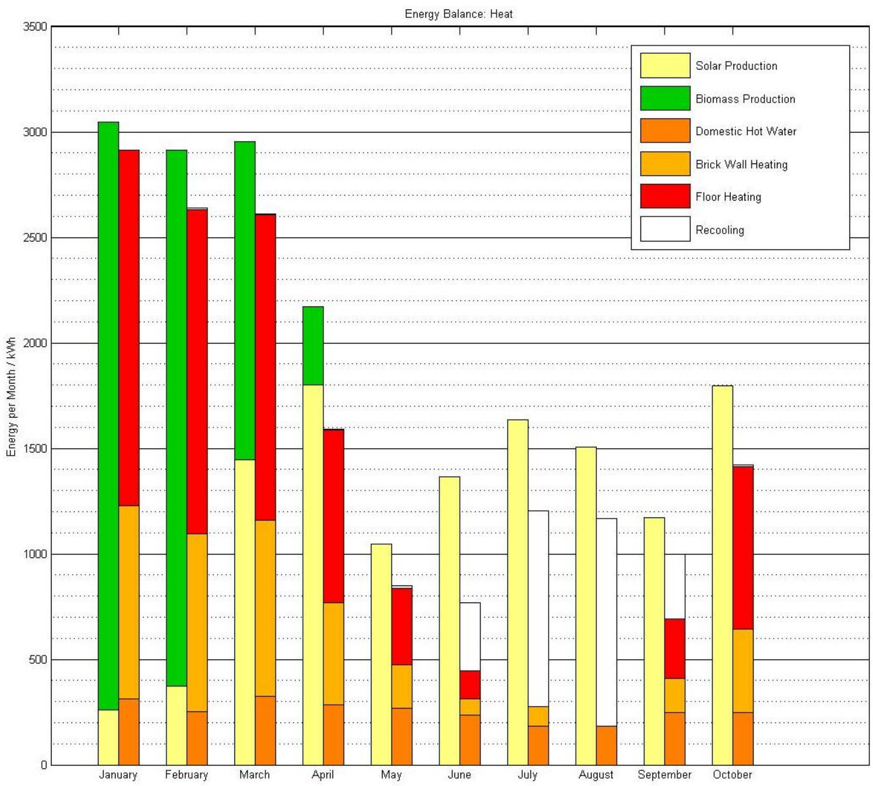

Figure 9: Heat energy balance. The left columns show the production, the right ones the consumption.

The energy contributions are:

- Solar Heat Production - heat delivered by the solar collectors to the hot water tank measured by a heat meter in the solar circuit.
- Biomass Heat Production - the heat delivered by the biomass boiler to the hot water tank measured by an energy meter in the biomass boiler circuit (cf. *Figure 10*).
- Brick Wall Heating - the thermal energy that is delivered to the thermally activated brick walls for heating from the hot water tank, measured by an energy meter in the circuit for all brick walls.
- Floor Heating - the thermal energy delivered to the floor heating from the hot water tank, measured by an energy meter in the circuit for all heated floors.
- Domestic Hot Water - the thermal energy delivered to the domestic hot water preparation from the hot water tank, measured by an energy meter installed in the circuit between the hot water tank and the heat exchanger.
- Recooling - the heat transferred from the hot water tank back to the ambient. This procedure is necessary to avoid stagnation of the solar system when the capacity of the hot water tank is exhausted. The energy for recooling is calculated by integrating the negative power readings of the appropriate energy meter. This energy meter is installed in the solar circuit.

	Production [kWh]		**Consumption [kWh]**			
	Solar Heat	**Biomass Heat**	**Brick Wall Heating**	**Floor Heating**	**Domestic Hot Water**	**Recooling**
Jan	262.0	2783.0	914.0	1684.7	313.0	2.1
Feb	371.0	2541.0	839.0	1540.0	254.0	4.3
Mar	1447.0	1508.0	834.0	1449.0	325.0	4.5
Apr	1799.0	371.0	482.0	819.0	286.0	5.7

May	1045.0	0.0	206.0	362.0	269.0	12.6
Jun	1365.0	0.0	76.0	132.0	237.0	324.1
Jul	1637.0	0.0	96.0	0.0	182.0	924.1
Aug	1506.0	0.0	0.0	0.0	184.0	982.2
Sep	1171.0	0.0	160.0	284.0	248.0	305.3
Oct	1798.0	0.0	394.0	771.0	249.0	6.5
sum	19604 kWh		16161.2 kWh			

Table 2: Heat energy balance.

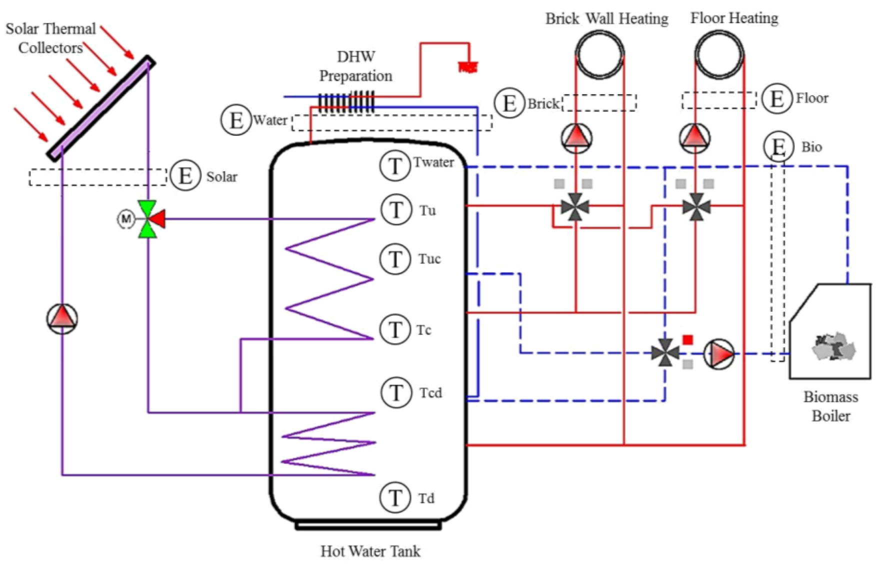

Figure 10: Schematic of the solar thermal system with relevant data nodes from the monitoring system. (Source: SCHUSTER GmbH & Co. KG, 2012)

3.3 Thermal Comfort

According to ANSI/ASHRAE Standard 55-2013, Thermal Environmental Conditions for Human Occupancy (ANSI/ASHRAE Standard 55) a thermal comfort is the condition of mind that expresses satisfaction with the thermal environment and is assessed by subjective evaluation. In this section the thermal comfort analyses based on the humidity level and indoor temperature are being presented. A comfort definition according to the German standard DIN

1946 II (DIN 1994) was selected. The following analysis simplifies this definition by taking the outer limits of this comfort field. Furthermore the operative temperature from the standard is interpreted as air temperature because of the lack of temperature data of all surfaces. Together with the relative humidity and the specific humidity SH_{air} of the air the comfort field is defined by following limiting conditions:

T_{air} > 20°C; T_{air} < 27°C; RH_{air} > 30%; RH_{air} < 65% and SH_{air} < 11.5 g/kg.

The analysis of each monitored month is being presented. The presented periods are from January to October 2013. The area which is analyzed is the living room (cf. *Figure 11*), children rooms (cf. *Figure 13* and *Figure 14*) and bedroom (cf. *Figure 12*).

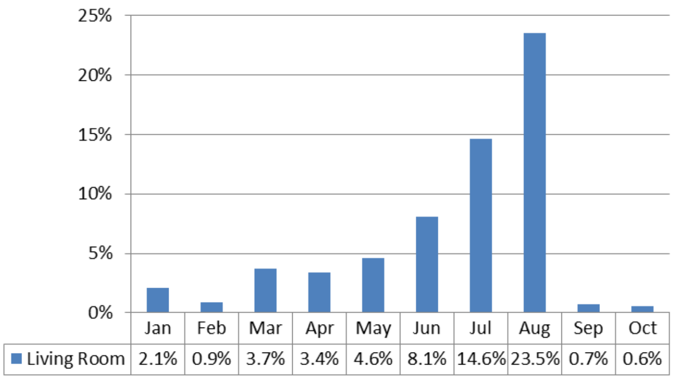

Figure 11: Monitored values outside of the comfort region in the living room in %.

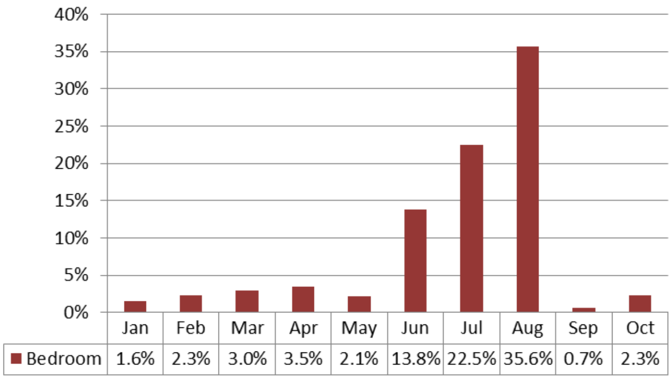

Figure 12: Monitored values outside of the comfort region in the bedroom in %.

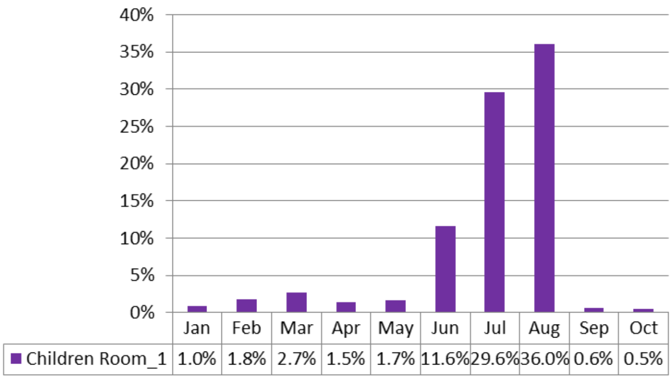

Figure 13: Monitored values outside of the comfort region in the children room_1 in %.

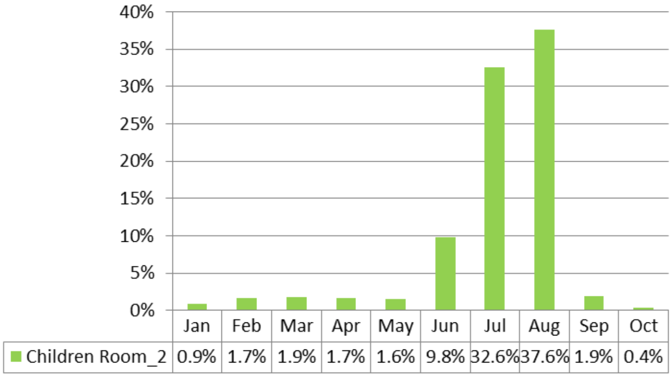

Figure 14: Monitored values outside of the comfort region in the children room_ 2 in %.

The thermal comfort scope defined by German standard DIN 1946 II with recorded values placed on its range for each month in the living room are presented in *Figure 15* through *Figure 24*.

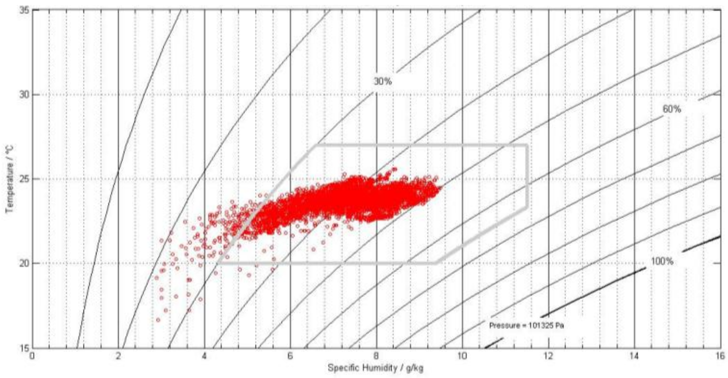

Figure 15: Comfort scope of the living room in January 2013. The room air parameters are outside the comfort region for 2.1% of the monitored time.

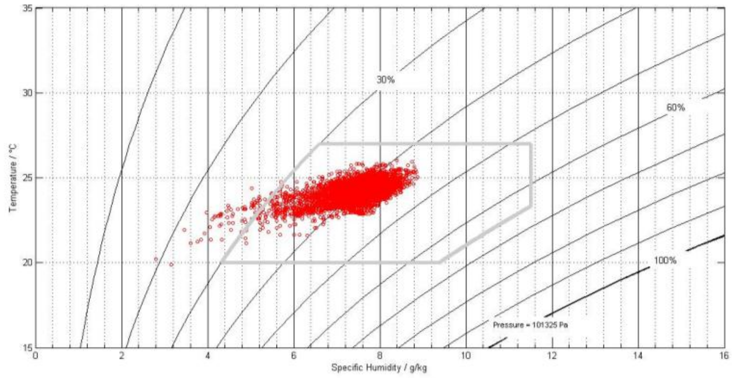

Figure 16: Comfort scope of the living room in February 2013. The room air parameters are outside the comfort region for 0.9% of the monitored time.

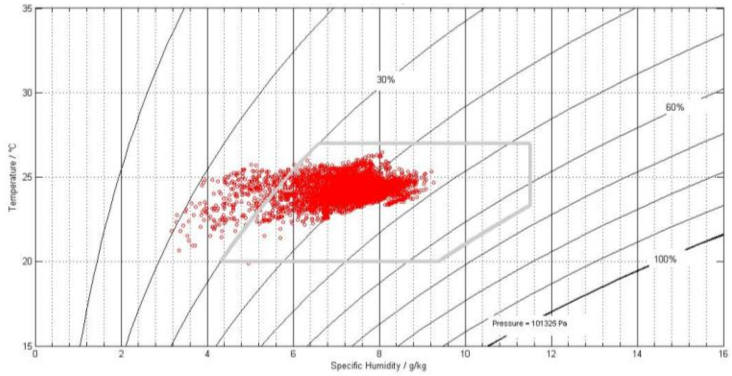

Figure 17: Comfort scope of the living room in March 2013. The room air parameters are outside the comfort region for 3.7% of the monitored time.

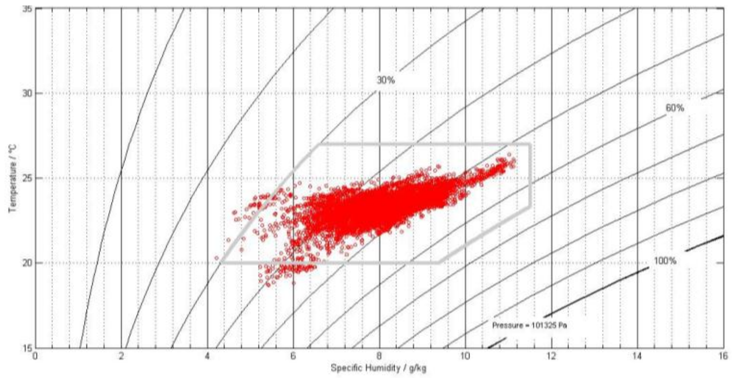

Figure 18: Comfort scope of the living room in April. The room air parameters are outside the comfort region for 3.4% of the monitored time.

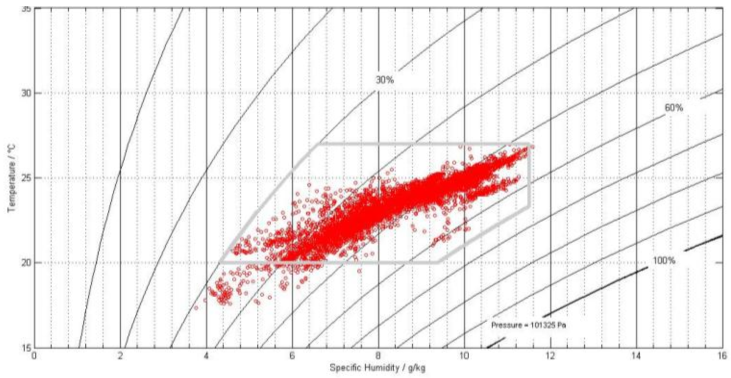

Figure 19: Comfort scope of the living room in May. The room air parameters are outside the comfort region for 4.6% of the monitored time.

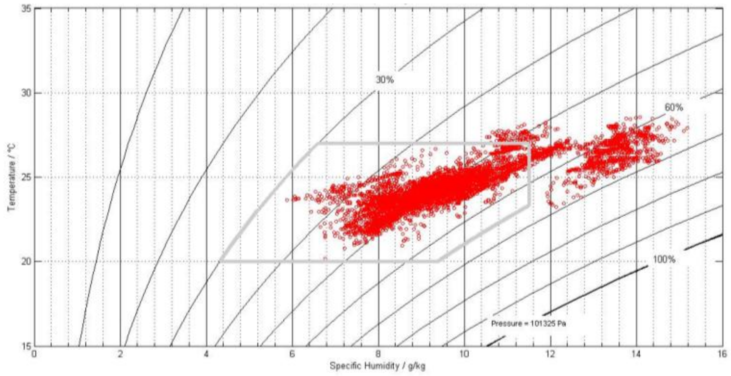

Figure 20: Comfort scope of the living room in June 2013. The room air parameters are outside the comfort region for 8.1% of the monitored time.

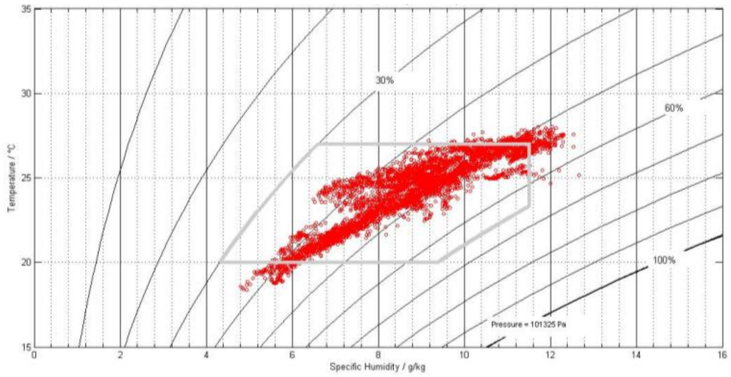

Figure 21: Comfort scope of the living room in July 2013. The room air parameters are outside the comfort region for 14.6% of the monitored time.

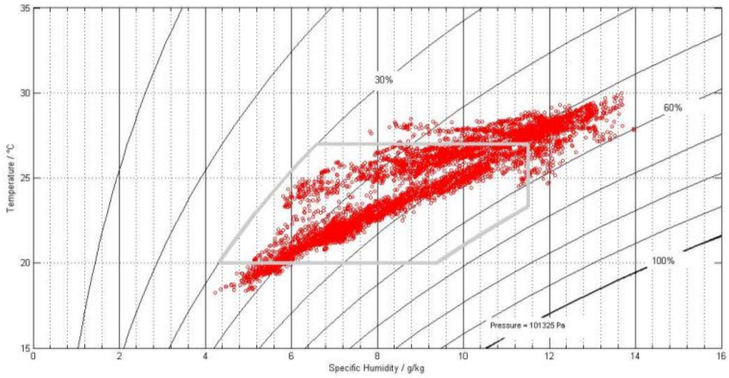

Figure 22: Comfort scope of the living room in August. The room air parameters are outside the comfort region for 23.5% of the monitored time.

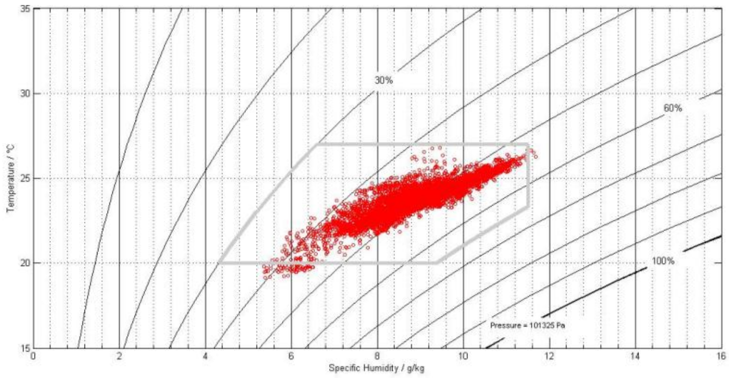

Figure 23: Comfort scope of the living room in September. The room air parameters are outside the comfort region for 0.7% of the monitored time.

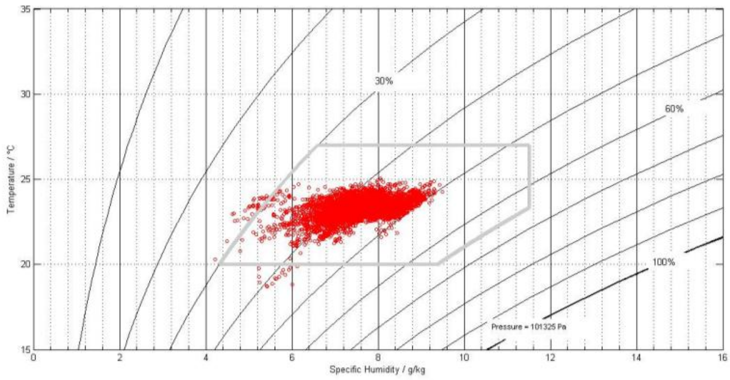

Figure 24: Comfort scope of the living room in October. The room air parameters are outside the comfort region for 0.6% of the monitored time.

Table 3 shows the percentage of all recorded values per months which are outside of the comfort region defined by German standard DIN 1946 II per particular room. *Figure 25* visualizes the data mentioned above.

Monitored values outside of the comfort region in %										
	Jan	Feb	Mar	Apr	May	Jun	Jul	Aug	Sep	Oct
Living Room	2.1	0.9	3.7	3.4	4.6	8.1	14.6	23.5	0.7	0.6
Bedroom	1.6	2.3	3.0	3.5	2.1	13.8	22.5	35.6	0.7	2.3
Children Room1	1.0	1.8	2.7	1.5	1.7	11.6	29.6	36.0	0.6	0.5
Children Room2	0.9	1.7	1.9	1.7	1.6	9.8	32.6	37.6	1.9	0.4

Table 3: *Monitored values outside of the comfort region per particular room in %.*

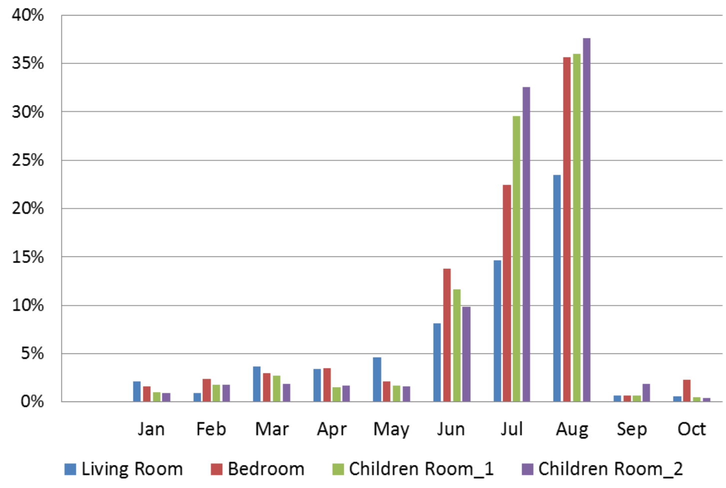

Figure 25: Monitored values outside of the comfort region in all the rooms in %.

4 CREATION OF THE BUILDING MODEL

4.1 Overview

The design phase model of the brick made *Sonnenhaus* building was implemented by AIT (Austrian Institute of Technology) in the simulation environment TRNSYS17. The model contains the building geometry and the physical values of the construction materials, based on architectural documentation of the existing building. The documentation contains precise information about building dimensions, construction materials and structural elements.

For the thermal simulation in the software environment, the established internal conditions were defined. The ventilation was implemented as constant air change rate of 0.17ACH. The heating was modeled as the ideal heating (unlimited heating power), with the constant temperature set point of 20°C. The model had a defined non-heating period from the first of May until the first of October, with no heating even when room temperatures drop below a specified value. No internal gains (such as persons' presence or lighting) and infiltration rate were defined. The first digital model created in the design phase uses semi-synthetically generated weather file which is based on actual historical metrological measurements from the past 30 years of the weather station in the area of the building site.

4.2 Building Envelope

The design phase model of the building envelope contains the data of the building geometry and the construction materials based on existing building documentation. The thermally activated brick walls were implemented as well. Construction of the building components and thermal conductivity values, thickness, heat capacity and density values of the building materials used in the simulation tool are presented in *Table 4* through *Table 9*.

Floor on the ground				
Material	**Thickness [m]**	**Thermal Conductivity [W/(m·K)]**	**Heat capacity [kJ/(kg·K)]**	**Density [kg/m^3]**
XPS TOP 30	0.2	0.036	1.45	200
Reinforced concrete	0.25	2.5	1.08	2300
Polystyrene concrete	0.1	0.06	1.24	600
Rolljet	0.03	0.038	1.4	15
Screed	0.07	1.7	1.08	2000
Flooring	0.02	1	2.2	600

Table 4: Physical properties of the floor construction.

Ceiling				
Material	**Thickness [m]**	**Thermal Conductivity [W/(m·K)]**	**Heat capacity [kJ/(kg·K)]**	**Density [kg/m3]**
Flooring	0.02	1	2.2	600
Screed	0.07	1.7	1.08	2000
Rolljet	0.03	0.038	1.4	15
Polystyrene concrete	0.1	0.06	1.24	600
Reinforced concrete ceiling	0.25	2.5	1.08	2300
Plaster	0.005	0.7	1.1	1600

Table 5: Physical properties of the ceiling construction.

External Wall				
Material	**Thickness [m]**	**Thermal Conductivity [W/(m·K)]**	**Heat capacity [kJ/(kg·K)]**	**Density [kg/m^3]**
External Plaster	0.03	0.8	1.116	1800
Porotherm 44	0.44	0.066	0.92	634
Plaster	0.005	0.7	1.1	1600

Table 6: Physical properties of the external wall construction.

Internal Wall				
Material	**Thickness [m]**	**Thermal Conductivity [W/(m·K)]**	**Heat capacity [kJ/(kg·K)]**	**Density [kg/m^3]**
Plaster	0.005	0.7	1.1	1600
Porotherm 12	0.12	0.066	0.92	634
Plaster	0.005	0.7	1.1	1600

Table 7: Physical properties of the internal wall construction.

Roof				
Material	**Thickness [m]**	**Thermal Conductivity [W/(m·K)]**	**Heat capacity [kJ/(kg·K)]**	**Density [kg/m^3]**
Ventilated roof	0.024	0.12	2.3	500
Rafter	0.2	0.12	1.61	700
Mineral wool	0.2	0.039	0.84	140
Rafter	0.1	0.12	1.61	700
Mineral wool	0.1	0.039	0.84	140
Rafter	0.024	0.12	1.61	700
Air gap	0.024	0.167	0.84	140
Plasterboard	0.015	0.25	1.05	900

Table 8: Physical properties of the roof construction.

Windows	
U-value of the window	0.8 W/m^2K
U-value of the frame	0.9 W/m^2K
G- value (Solar Heat Gain Coefficient)	0.5

Table 9: Physical Properties of Simulation Materials.

4.3 Weather data

One of the crucial inputs for the simulation is the weather data. The vital information for this simulation is ambient air temperature, ambient relative humidity, diffuse, and global and beam radiation on the horizontal surface. Accurate weather data plays an important role in the model calibration process and the thermal simulation since it captures relevant microclimate variations.

In the design phase model created by AIT, a semi-artificial weather file was used. This file was based on actual historical metrological measurements recorded in the past 30 years from the weather station in the area of the building site (Selke et al. 2012).

The new weather file, which is used for the calibrated model of the simulation was generated and delivered by ZAMG (Zentralanstalt für Meteorologie und Geodynamik). The sensors that are used by ZAMG are being presented in the appendix *Table 20*. The ZAMG weather station is situated 3.5 km from the building, at latitude 15°12'13" and longitude 48°37'04" (cf. *Figure 26*).

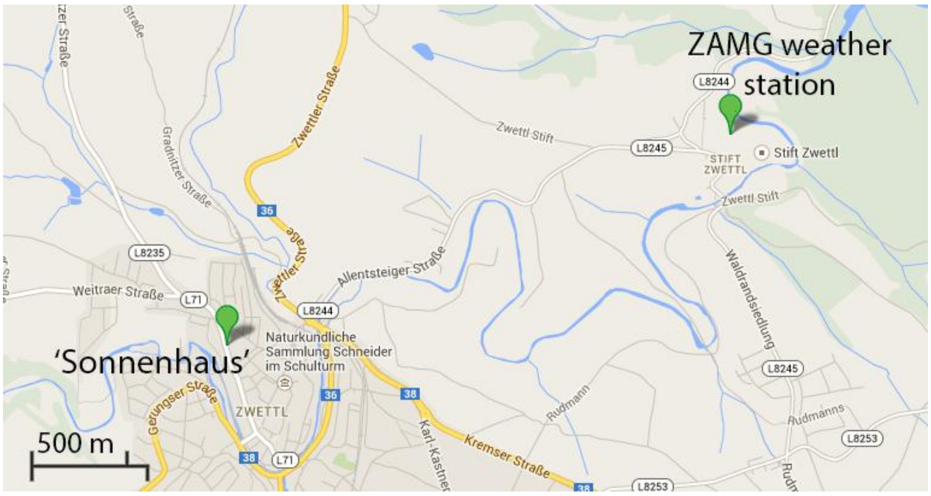

Figure 26: Location of the building and the ZAMG weather station. (Source: Google Maps)

In order to visualize the relation the effect of outside air temperature on building energy consumption, a simplified representation of outside air-temperature data in the form of *degree days* is presented.

Heating degree days (HDD) are a measure of how much (in degree Celsius), and for how long, the outside air temperature was below a base temperature. The base temperature represents the temperature below which the building needs heating. This is typically set to 15.5°C in the Europe for most buildings.

Heating degree days are intended to represent the value of the thermal load requirements to maintain the interior dwelling temperature when exterior temperatures are lower than interior temperatures (Bromley 2008).

In order to calculate the HDD for historical weather data and ZAMG weather file the approximation method was introduced. The average daily temperatures were calculated, and subtracted from the base temperature which was designed to 15.5 degree. If the value is less than or equal to zero, that day had zero HDD. If the value is positive, that number represents the number of HDD on that day. For each month, the daily HDD values were summed up.

Figure 27 and Figure 28 show the significant differences of the major weather parameters between the two sets of monthly data for the semi- synthetically generated weather file and the ZAMG data.

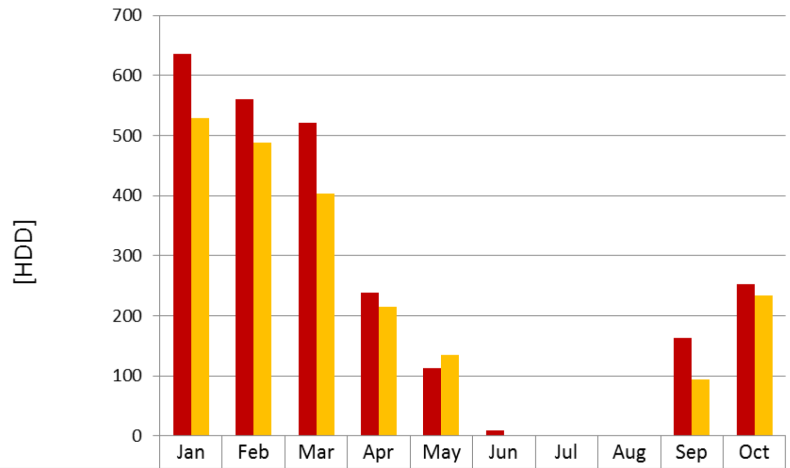

	Jan	Feb	Mar	Apr	May	Jun	Jul	Aug	Sep	Oct
Semi- synthetically generated weather data	636	561	522	239	113	9	0	0	164	252
ZAMG	528	488	402	214	134	0	0	0	93	234

Figure 27: Comparison of heating degree days (HDD) between ZAMG and semi-synthetically generated weather data.

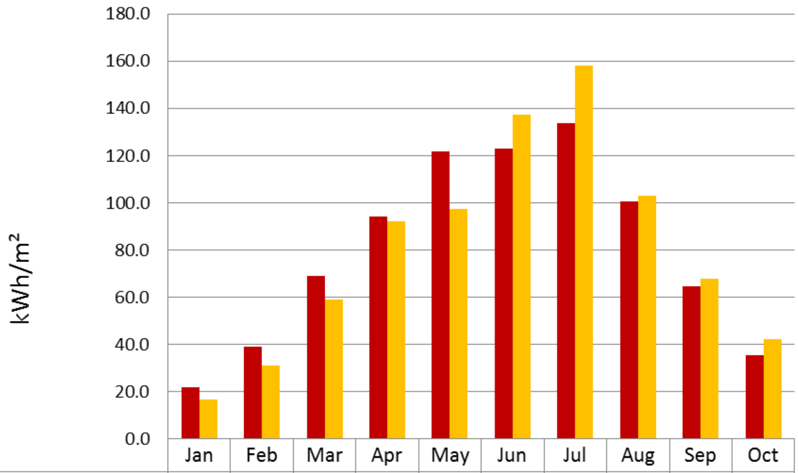

	Jan	Feb	Mar	Apr	May	Jun	Jul	Aug	Sep	Oct
Semi- synthetically generated weather data	22.0	39.0	69.0	94.0	121.7	122.8	133.7	100.8	64.8	35.7
ZAMG	16.9	31.0	59.2	92.1	97.3	137.4	158.1	103.0	67.9	42.5

Figure 28: Comparison of solar radiation on a horizontal surface in kWh/m² between ZAMG and semi- synthetically generated weather data.

The temperature statistics for the semi- synthetically generated weather data are presented in the *Figure 29*. *Figure 30* shows the temperature statistics for the weather data generated and delivered by ZAMG weather station (cf. *Figure 26*).

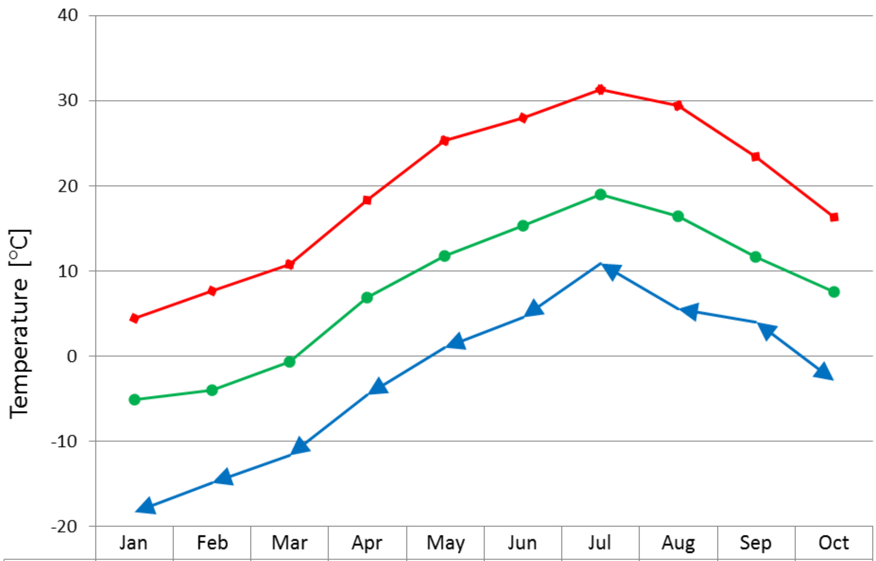

	Jan	Feb	Mar	Apr	May	Jun	Jul	Aug	Sep	Oct
Max	4.5	7.7	10.8	18.4	25.4	28	31.4	29.5	23.5	16.4
Avg	-5.0	-4.0	-0.7	6.9	11.8	15.3	19.0	16.4	11.6	7.5
Min	-18.2	-14.8	-11.6	-4.5	1.1	4.6	11	5.6	4.1	-2.8

Figure 29: Monthly temperatures of the semi- synthetically generated weather data..

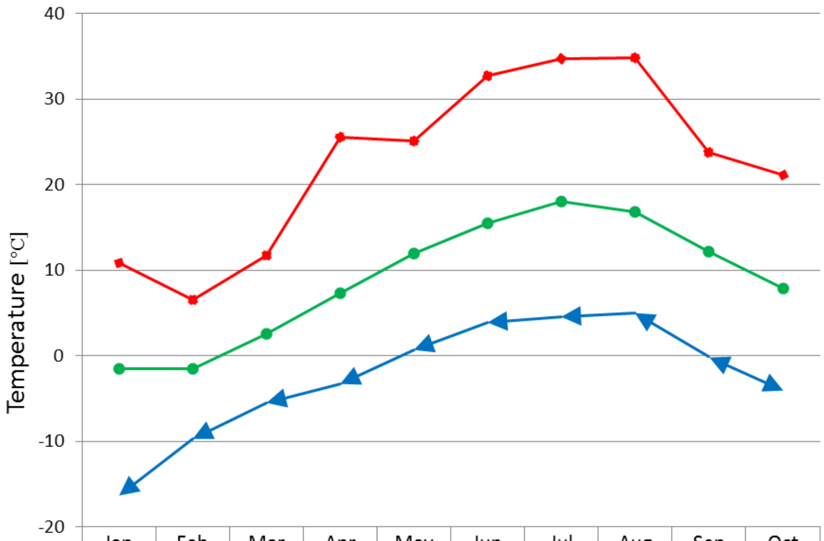

	Jan	Feb	Mar	Apr	May	Jun	Jul	Aug	Sep	Oct
Max	10.9	6.6	11.8	25.6	25.1	32.7	34.7	34.9	23.8	21.2
Avg	-1.5	-1.4	2.6	7.3	11.9	15.5	18.0	16.8	12.1	7.8
Min	-16.3	-9.7	-5.5	-3.3	0.6	3.8	4.5	5	-0.1	-4

Figure 30: Monthly temperatures recorded by ZAMG.

Definitions for temperature statistics presented in *Figure 29* and *Figure 30* are the following:

- Max - the highest by month maximum air temperature observed at the site (°C).
- Avg- the average monthly air temperature observed at the site, calculated over the month (°C).
- Min- the lowest by month minimum air temperature observed at the site (°C).

5 DEFINITION OF THE BUILDING REGIME

5.1 Overview

The building regime represents established conditions, internal heat gains, and conditioning. The goal of this chapter is to define the building regime based on the monitored conditions, which were affected virtually by occupants. Subsequently this model with implemented regime based on the monitored conditions will be defined as *Final Model* and the results of its thermal simulation as a *Final Simulation.*

As introduced before the occupants play several roles in determining a building's energy use and have a strong influence on the energy performance of the building. Occupants indirectly use energy as beneficiaries of heating systems, lighting systems, water systems, and other building services. They also interact with a building to enhance their personal comfort by heating or ventilating (C.J. Andrews, 2013).

In order to reconstruct the model of the existing building and analyze the thermal performance under the operative conditions during the whole monitoring period, the building regime was defined.

The variables, which are considered to define the building regime, are:

- heating set points – the temperature of the zone, manually defined by the occupants
- building occupancy level and profile – the amount of the occupants per zone and the periodicity of their occurrence
- natural ventilation – openings the windows by the occupants
- lighting power level and profile – determines when and which type of the lights were used in the rooms where the occupants were present

The definition of the input parameters was based on the available data which was monitored during the observation time range. The precise implemented methods used to generate the required input parameters and their descriptions are presented in the following sections.

5.2 Heating

A heater is an object that emits heat or causes another body to achieve a higher temperature. In the *Sonnenhaus* the heat is emitted by the thermally activated walls and floors.

In order to control indoor air, the walls and the floors are defined as an active heating layer. The heating requirements of every zone are defined as idealized heating and distributed to the walls and floors of the zones. The model does not heat each of the construction parts separately but directly heats up the air in particular zones. The temperature set for the heating equipment is related to the air temperature of the zone. The temperature in each zone was controlled by the occupants manually. The nominal values of the temperatures in each room were defined in hourly intervals, based on the recorded values of the monitoring system.

The data gaps of the monitoring system (cf. Chapter 3.1) were filled with the average temperatures for each zone from the former recorded values, with corresponding similar outdoor conditions were introduced.

Table 10 presents statistics of the recorded temperature values. These were calculated from hourly measurements over a time period of ten months, except the some gaps (cf. *Table 1*).

	Corridor	**Staircase**	**Living Room**	**Bedroom**	**Child Room 1**	**Child Room 2**	**Bathroom**
Max. Value [°C]	28.5	29.0	29.3	29.4	29.8	29.8	29.8
Min. Value [°C]	19.3	21.5	17.9	12.2	13.5	15.8	18.1
Avg. Value [°C]	23.4	24.1	24.0	23.5	23.8	23.7	24.8
SD (σ)	1.3	1.3	1.4	1.8	1.6	1.7	1.4

Table 10: Documentation of recorded temperature values.

5.3 Ventilation

The building model defines the natural ventilation, which requires no mechanical device to work. The airflow is driven by the draft due to temperature or pressure differences between inside and outside. The warm air inside the building is less dense than the cooler air outside, and thus tries to escape from windows openings high up in the building envelope. Cooler, denser air enters through openings lower down. This process continues if the air entering the building is continuously heated, typically by casual or solar gains. Natural ventilation as an alternative to mechanical ventilation has several benefits: low running cost, zero energy consumption, low maintenance and probably lower initial cost. It is also regarded as healthier, having less hygienic problems with ducts, and filters. Furthermore the 'naturalness' in the way that it connects with outside, often in conjunction with windows, is seen as a psychological benefit (Baker 2013). However the natural ventilation depends on outside climatic conditions and is difficult to control. There is a possibility of having a high air change rate during certain unfavorable climate conditions and this might cause big thermal losses and leads to high heating demand.

In order to create the input parameters for the air change rate in the building simulation, the *active tracer gas measurement* using *decay concentration* method is introduced. In our case, it is not possible to avoid noise in data from unknown activities and occupancy in the room. Therefore it is very difficult to properly define the natural ventilation rate with concentration decay method. Especially during the warm months we have insufficient information of how long the windows were opened, since the CO_2 decay curve will not decline to zero but to the values which are near to the ambient CO_2 values (Laussmann 2011). Additionally although after CO_2 is released in a room as exhaled breath its concentration can decay exponentially through the opened window, but still, the further CO_2 supply can still occur, since during the entire procedure the room might be occupied (Bekö et al. 2011).

In order to estimate the average air change rate for one hour, the 5 minutes stamps of recorded data were taken into account. Only if the decay of the CO_2 level lasting for more than 3 measurements in the row was notice, the air change rate with the decay trace gas method was introduced. (Equation (1)) For the measurements where the CO_2 levels were increasing, no ventilation was assumed, therefore the 5 minute interval in those cases was set to 0. All calculated values over summed up and the average hourly value was calculated, since for the simulation input the hourly value of the air change rate is requested. *Figure 31* shows the example of average daily air change rate for a bedroom during the winter day.

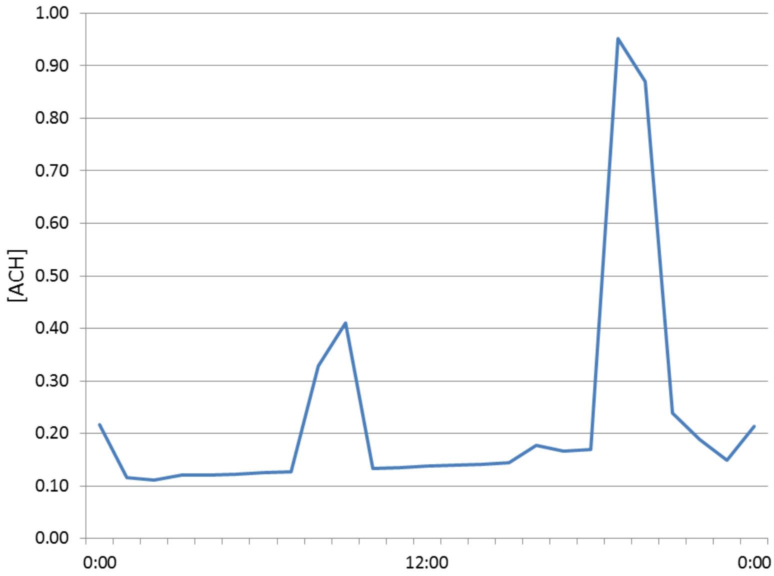

Figure 31: Air Change Rate (*ACH) for the winter day (2.02.2013).*

The calculated average air change rates for each zone, with a calculation based on the concentration decay method are presented in the Table 11.

Zone	**ACH [ac/h] average**	**ACH [ac/h] minimum**	**ACH [ac/h] maximum**
Living room+kitchen	0.33	0.02	1.03
Children room 1	0.27	0.02	2.23
Children room 2	0.29	0.02	2.34
Bedroom	0.24	0.02	2.62

Table 11: *Calculation of the air change rate based on CO_2 level.*

Due to many uncertainties this method was introduced just for the cold months, which are January, February, March, and October for the zones, where CO_2 sensors were installed. For the remaining months and zones, the values of the calculated air change rate requirement according to ASHRAE Standard 62-2001 were introduced.

Calculation of air change rate requirement according to minimum ventilation rates in breathing zone based on are presented in the *Table 12*.

Zone	**Volume [m^3]**	**Floor area [m^2]**	**ACH [ac/h]**
Living room	183.7	45.65	0.27
Office room	33.6	7.08	0.23
WC	10.9	2.53	0.25
Entrance hall	143.5	25.5	0.19
Kitchen	63.9	14.41	0.24
Children room 1	83.1	19.47	0.25
Children room 2	84.6	19.41	0.25
Bedroom	61.1	14.11	0.25
Bathroom	84.1	20.25	0.25
Corridor	72.1	13.16	0.20

Table 12: Calculation of the air change rate requirement according to ASHRAE Standard 62-2001

5.4 Infiltration

Infiltration is the unintentional or accidental introduction of outside air into a building, typically through leaks in the building envelope and through use of doors for passage. Infiltration is sometimes called air leakage. The leakage of room air out of a building, intentionally or not, is called exfiltration. Infiltration is caused by wind, negative pressurization of the building, and by the stack effect.

The infiltration rate is the volumetric flow rate of outside air into a building, typically defined in liters per second or in the air change rate. The air change rate (unit of 1/h) is the volume of the air that is exchanged and replaced by the fresh air in the room within 1 hour. The air change rate is also known as *air changes per hour* (ACH).

In order to measure the infiltration rate of the building, typically a non-intrusive method, such as the tracer-gas technique is used. There are three different methods of determination of the air change rate with the tracer-gas technique: *concentration decay*, *constant injection* and *constant concentration.* Due to available recorded data, the concentration decay method, where CO_2 is used as a tracer-gas was applied. In this method it is assumed that an amount of tracer-gas (CO_2), which was exhaled by occupants, was initially mixed into the room air and then the occupants left. This method requires that the tracer-gas concentration in the space has to be as uniform as possible for accurate measurement of the infiltration rate. Therefore the data from night periods was used in order to avoid noise in data from unknown activities and occupancy in the room.

The measurements took place during a winter night in the living room, downstairs, where the windows were closed and we were certain, that the occupants had left the room.

Comparing CO_2 to the other tracer gases such as Nitrous Oxide, Freon or Helium, it has the characteristic that there is always a certain amount of it in the outdoor air. Therefore the background concentration cannot be neglected but similar to the outdoor air concentration of CO_2 which varies between 350 ppm and 450 ppm. Depending on the season this value can be even higher. Therefore, the CO_2 decay curve will not decline to zero but to the values which are near to the ambient CO_2 values. This must be taken into account when analyzing CO_2 decay curves (Laussmann 2011).

Five measurements were carried out in order to define the infiltration rate. The first one was recorded on 2nd February 2013 at 21:00 with an initial tracer-gas concentration value of 620 ppm. At the end of the measurement period, on 3rd February 2013 at 5:00 the tracer-gas concentration at the last recorded value was 529.5 ppm. The observation time in total was 8 hours (cf. *Figure 32*).

From these measurements, the air change rate can easily be calculated by the formula given in the Equation (1).

$$A = (\ln C_1 - \ln C_2)/\Delta T \quad (1)$$

Where:

ln = natural logarithm

C_1 = Tracer gas concentration at start of test

C_2 = Tracer gas concentration at end of test

The result of the first observation was 0.0197ACH.

The second measurement which was used in order to define the infiltration rate was recorded on 27th February 2013 at 22:00 with the initial tracer gas concentration value of 631 ppm. At the last point of measurement on 28th February 2013 at 6:00 the tracer gas concentration was 421 ppm. The observation time was again 8 hours. The result of the second measurement was 0.0219.

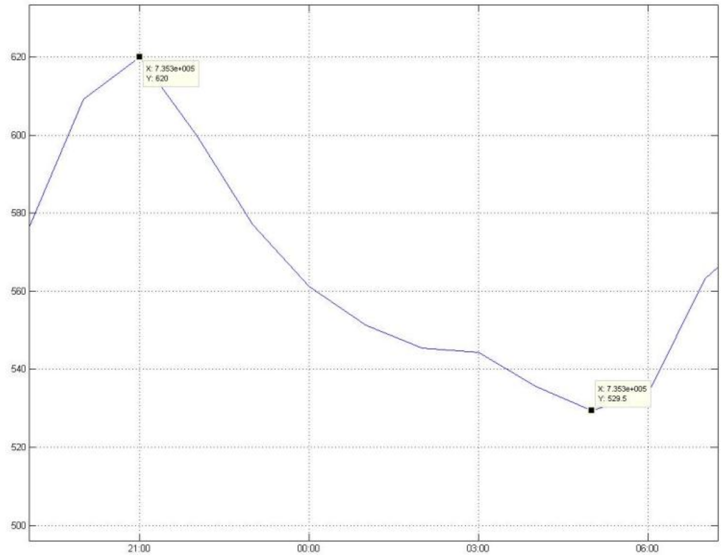

Figure 32.: CO2 decay curve.

The same calculations were provided for 3 other periods of time, with the same internal conditions- no occupants in the room closed windows. The results were equal to 0.0199, 0.0201and 0.0184 (cf. *Table 13*). The average value of these results, 0.02, was used in the simulation tool as an infiltration rate is equal to constant value of 0.02 air changes per hour.

measurement	**2.02.2013**	**27.02.2013**	**1.03.2013**	**4.03.2013**	**8.03.2013**
1st measurement	620 ppm	900 ppm	820 ppm	960 ppm	721 ppm
2nd measurement	529.5 ppm	755 ppm	699 ppm	834 ppm	646 ppm
observation time	8 h	8 h	8 h	7 h	6 h
[ACH]	0.0197	0.0219	0.0199	0.0201	0.0184

Table 13: Calculated infiltration rate based on the concentration decay method.

The building is designed to minimize the infiltration air in order to reduce heating energy costs. However, it cannot serve as a substitute for proper ventilation; therefore the natural ventilation via manually operable windows and other openings is necessary to ensure the appropriate air quality in the object.

5.5 Occupancy

The building energy performance is influenced by the occupants’ behavior through several factors (Brandemuehl 2011). Not only pollutants such as water vapor, carbon dioxide or odors are being emitted by each human being but also heat. This means that the occupants’ presence directly modifies the indoor environment and has a direct influence on the energy performance of the building (Andrews 2013).

In order to create an hourly schedule of occupancy for each of the living zones, the level of CO_2 was analyzed and applied to all rooms, where CO_2 sensors were installed: the living room, the bedroom and both children rooms.

The algorithm to guess the presence of people in a room from CO_2 levels (and changes thereof) was empirically developed and is outlined by the following rules: (cf. *Figure 33*)

- If the CO_2 level increases for two hours by at least 70 ppm and the values were increasing in the following measurement, then the occupancy was default as 1.
- If the difference of CO_2 level for two hours was lower than 70 ppm, the occupancy remains default as during the previous analyses.
- If the CO_2 level decreases for two hours by at least 70 ppm and the values were decreasing in the following measurement, then the occupancy was default as 0.

Exception was the bedroom and the living room, where the differences in the levels of the values of the CO_2 were much higher. There the algorithm to guess the presence of people in a room from CO_2 levels (and changes thereof) was empirically developed and is outlined by the following rules:

- If the CO_2 level increases for two hours by at least 70 but not more than 140 ppm and the values were increasing in the following measurement, then the occupancy was default as 1.
- If the CO_2 level increases for two hours by at least 140 ppm and the values were increasing in the following measurement, then the number of occupants was assumed to be equal to as 2.

- If the difference of CO_2 level for two hours was lower than 70 ppm, the occupancy remains default as during the previous analyses.
- If the CO_2 level decreases for two hours by at least 70 ppm and the values were decreasing in the following measurement, then the occupancy was default as 0.

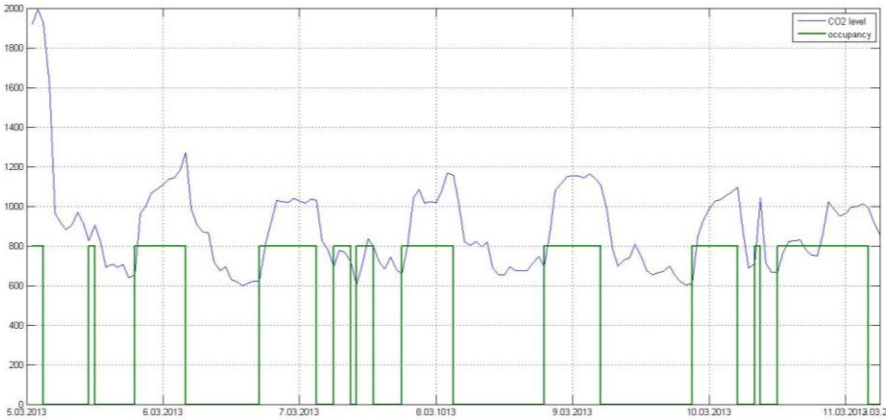

Figure 33: Visualisation of the calculated occupancy schedule from 5th March until 11th March in the child room.

Like in the case of the ventilation, due to many uncertainties this method was only applied for the cold months January, February, March, and October, where the CO_2 measurements are only insignificantly disrupted by the natural ventilation. For the dates, where we were not able to define the occupancy level based on CO_2, neither other information about occupancy was available, the standard occupancy schedules, based on the estimated occupancy patterns from two first weeks of March were created. The standard daily occupancy schedule for a weekday and a weekend-day are presented in *Figure 34* and *Figure 35*.

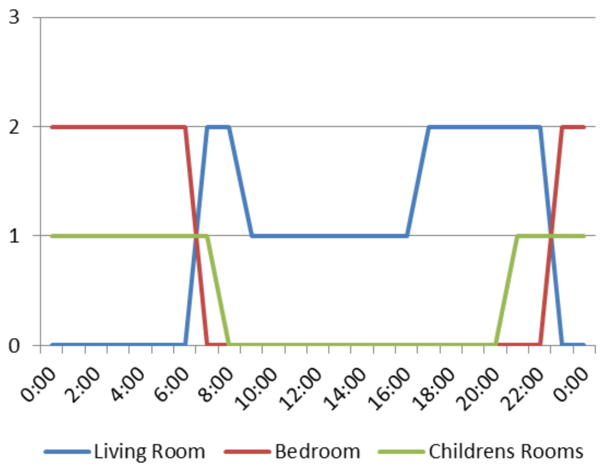

Figure 34: Standard daily occupancy schedule on a weekday.

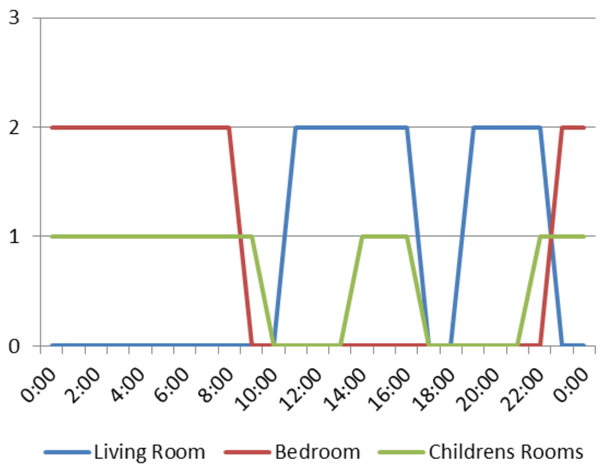

Figure 35: Standard daily occupancy schedule on a weekend.

5.6 Internal Gains

Internal gains can account for most heat gain in buildings. These gains are from occupants, lights and electric equipment. In this chapter this term only refers to the gains from lights, since the gains from occupants were already discussed in the previous chapter, and no data about electric equipment is available. Lighting has an indirect effect on the heating needs of the building through the heat generated by the lamps. (Brandemuehl et al. 2011)

Due to the lack of individual electricity measurements for each room, the monitored energy used for lighting was divided proportionally to the square meters of each room. In the simulation software, the number and types of lamps in each room were defined, and the energy from the monitoring system was set as an input data. In the first 2 months of 2013, which contained long data gaps, the missing values were substituted with averages of the first two months. The electricity meters were monitoring only the energy consumed by the lighting system; therefore due to the lack of additional data, the electrical equipment was not introduced in the simulation tool. The distribution of light bulbs in all rooms is presented in the *Table 14*.

Zone	**50 W (Halogen Lamp)**	**75 W (Incandescent light bulb)**
Living room	19	-
Office room	6	-
WC	3	-
Entrance hall	14	-
Kitchen	11	-
Children room 1	3	-
Children room 2	2	1
Bedroom	-	4
Bathroom	5	1
Corridor	6	2

Table 14: Light bulbs distribution.

6 RESULTS AND ANALYSIS

The *Final Model* is the calibrated model with the actual weather data from ZAMG used as input and with defined building regime, based on the monitored conditions, which were affected largely by occupants.

The *Design Phase Model* is the initial model, created in the early stage of the project during the building's planning phase. The *Design Phase Model* represents the expected behavior without any feedback regarding the real implementation of the building, the specific weather or the individual user behavior. In this model, the input data are the set values for the room temperature of 20°C, a non-heating period defined from 1st May to 1st October and an air change rate for ventilation as a constant value of 0.17 ACH. The modeling of the design phase uses the semi- synthetically generated weather data file and in this model no internal gains and no infiltration were defined.

This chapter presents the simulation results of the *Final Model* and compares them to the recorded values of the monitoring system as well as to the first model from the *Design Phase* (called *Design Model* in the following). Explanations of the observed differences are discussed and the impact of particular parameters in the simulation is analyzed.

6.1 Accuracy of the Simulation Results

In order to present the simulation results and to check their accuracy, we show the difference between the exact, monitored value of consumed energy *(Monitoring)* and the value of the energy calculated in the *Final Model*. *We* also present the difference between *Monitoring* and the *Design Phase.*

The analysis is done by evaluating the absolute and relative errors, which are defined by Equation (2) and Equation (3):

$$e_a = (V_s - V_m) \quad (2)$$

$$e_r = (V_s - V_m) / V_m \cdot 100\% \quad (3)$$

Where:

e_a = absolute error

e_r = relative error

V_m = value from the monitored data (“true value”)

V_s = simulation result

Comparing the *Design Phase* model with the actual, monitored building performance (*Monitoring*) very big underestimation of the heating demands over the whole year (except the first month) can be observed. In the *Design Phase*, only heating demands for the months January, February, March, April and October were planned, while the monitoring showed demands for all months except August. Comparing the *Final Simulation* with the *Monitoring*, minor overestimation of the heating energy in the first three months (January, February and March) can be observed. Furthermore, the *Final Simulation* provides data the whole monitored period, except the months July and August (cf. Figure 36).

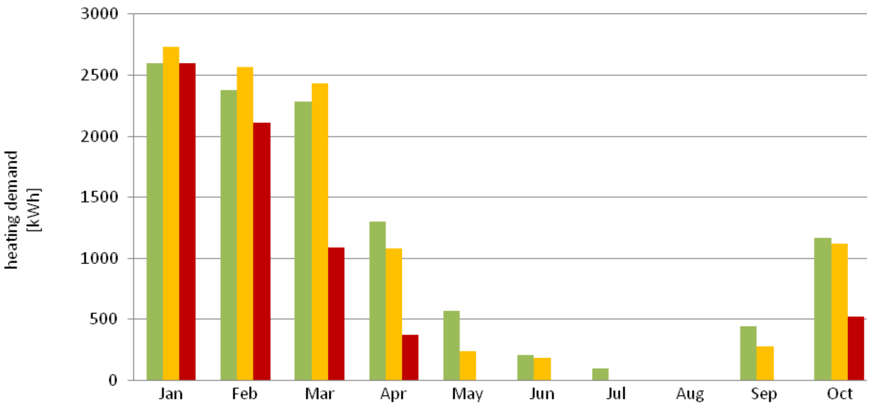

	Jan	Feb	Mar	Apr	May	Jun	Jul	Aug	Sep	Oct
Monitoring	2598.7	2379.0	2283.0	1301.0	568.0	208.0	96.0	0.0	444.0	1165.0
Final Simulation	2734.7	2569.0	2435.3	1076.6	235.7	185.2	0.0	0.0	275.9	1120.3
Design Phase	2598.1	2106.7	1084.4	370.2	0.0	0.0	0.0	0.0	0.0	520.9

Figure 36: Monitoring, Design Phase and Final Simulation- comparison.

Figure 37 highlights the absolute error of the *Design Phase* and the *Final Model*. The *Design Phase* model differs from the *Monitoring* by an absolute error in monthly evaluation varying between -1189.6 kWh and -0.6 kWh. For the *Final Model*, the absolute error varies between -332.3 kWh and 190 kWh.

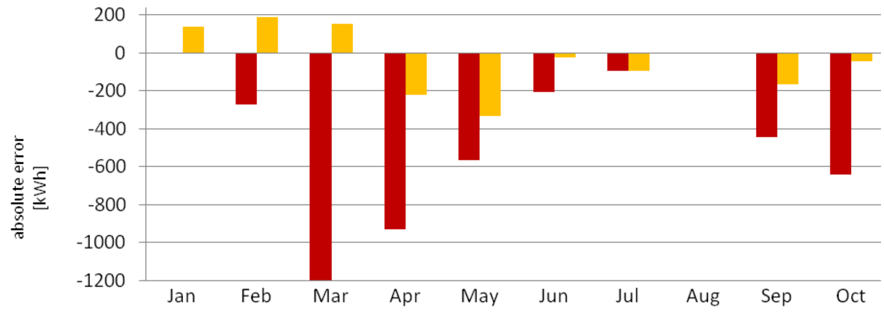

	Jan	Feb	Mar	Apr	May	Jun	Jul	Aug	Sep	Oct
Design Phase /Monitoring	-0.6	-272.3	-1198.6	-930.8	-568.0	-208.0	-96.0	0.0	-444.0	-644.1
Final Model /Monitoring	136.0	190.0	152.3	-224.4	-332.3	-22.8	-96.0	0.0	-168.1	-44.7

Figure 37: Monthly heating demand absolute error of simulation results of Design Phase Model, Final Simulation and Monitoring.

Figure 38 shows the relative error of these two models. Note that these values are not meaningful during the warm months, where either the monitoring data or the model data (or both) are zero or near-zero. Nevertheless, it can be seen how the *Final Model* outperforms the *Design Phase*.

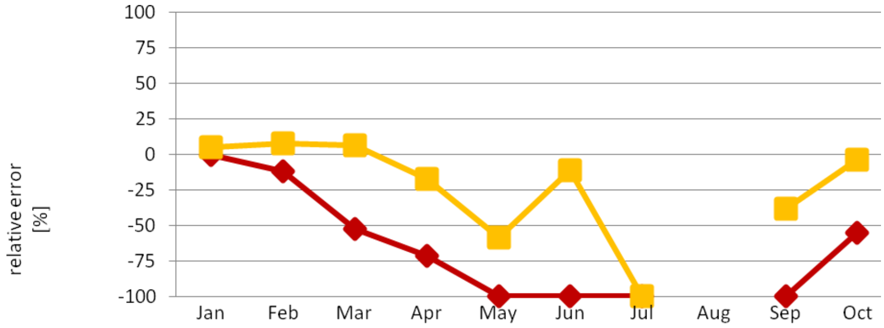

	Jan	Feb	Mar	Apr	May	Jun	Jul	Aug	Sep	Oct
Design Phase /Monitoring	0.0	-11.4	-52.5	-71.5	-100.0	-100.0	-100.0		-100.0	-55.3
Final Model /Monitoring	5.2	8.0	6.7	-17.2	-58.5	-11.0	-100.0		-37.9	-3.8

Figure 38: Monthly heating demand relative error of simulation results of Design Phase Model, Final Simulation and Monitoring.

Due to software limitations, the *Final Model* neglects the heat stored in the building mass, spatial temperature distribution of room air and the heat transfer to room air from the hot water tank.

The possible reasons for the deviations of the *Final Model* compared to the monitored values and an analysis of eventual additional factors are presented in the following subsections.

External Shades

Each of the windows has its own external shade and it is controlled by the occupants manually. In addition to this, shades impact on the lighting demand, which can lead to minor differences in the internal heat gains. However, there was no monitoring system for the external shades. Therefore, in the simulations the simultaneous impact of shading devices and the shading control was not taken into account. It might have reduced the solar gains, especially during the sunny months, and at the same time increased the heating demands.

Night Ventilation

As was discussed, we were not able to precisely define the natural ventilation air change rates, since the velocity of the air was not measured. The windows might have been opened for a longer time, and the ACH could be higher than the default values that were introduced in the simulation tool. This results presumably in higher heating demands, especially in the time period where default ventilation values were introduced (April, May, June, July, August, and September).

Heating System Efficiency

Lastly, the model for the heating demand uses an idealized heating unit with unlimited power. This results in a different time behavior compared to the implemented brick wall and the floor heating.

6.2 Sensitivity Analysis

In this chapter the particular influence of individual factors on the simulation model will be analyzed. Therefore, five different simulation models were created, briefly denoted as *Ver1*, *Ver2*, *Ver3*, *Ver4*, and *Ver5*. Each of them equals the *Final Model*, with one detail omitted or simplified. The factors respectively stand for semi-synthetical weather file, set heating point 20°C, no infiltration rate, no internal gains and ventilation value set to 0.17 ACH (cf. *Table 15*).

Short Name	Name	Description
Ver1	Semi-synthetical weather file	Semi-synthetically generated weather file is used instead of ZAMG weather data.
Ver2	Set heating point 20°	A constant temperature of 20°C is used as heat set point instead of different temperature values default by the users.
Ver3	No infiltration rate	The infiltration rate is not defined.
Ver4	No internal gains	The internal heat gains are not defined.
Ver5	Ventilation value set to 0.17 ACH	The ventilation rate is set to constant value of 0.17 ACH.

Table 15*: Variety of simulated models with descriptions.*

For presenting the simulation results and to check their impact, we show the difference between the exact, monitored value of delivered energy *(Monitoring)* and the value of the energy calculated in the different design scenarios results *(Ver1, Ver2, Ver3, Ver4, Ver5).* In order to see how the particular factors influence the simulation, we also show the differences between the *Final Model* results and different design scenarios.

Based on this sensitivity analysis we are able to indicate the most influencing factors of the thermal simulation and check which scenario is most accurate.

Weather Data

On-site weather data are not easy to obtain and therefore in many simulations historical or artificially generated data are used as input for the models. As observed, the simulation result with average data is different from the result with the actual weather data.

The *Monitoring* results were compared with the simulation of the *Ver1*. This model equals the *Final Simulation* except for the weather file, which was substituted with the semi-synthetically generated weather data.

We can observe that the heating degree days impact the heating energy demand and consumption more than global horizontal irradiance at the low bin levels.

The results of the comparison of the *Ver1* model and *Monitoring* shows that the energy consumption values predicted by *Ver1* were consistently higher in the winter months than the measured energy consumption, although the users' behavior and actual building regime was already taken into account. We can also observe underestimation of the heating demand in the summer months.

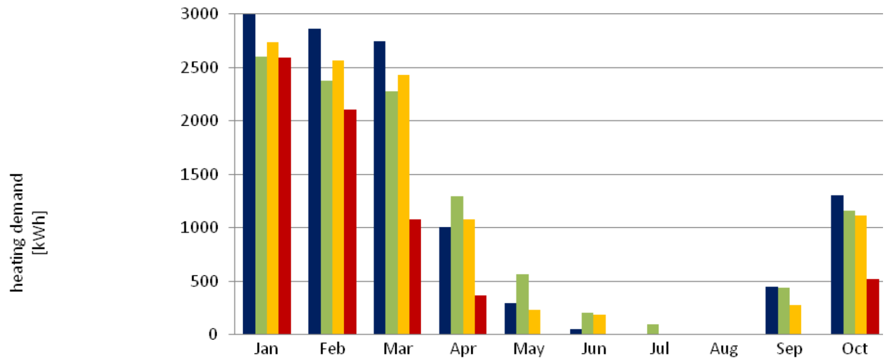

	Jan	Feb	Mar	Apr	May	Jun	Jul	Aug	Sep	Oct
Semi-artificial Weather Data	3073.7	2865.1	2750.3	1007.1	300.2	52.3	0.0	0.0	450.0	1303.7
Monitoring	2598.7	2379.0	2283.0	1301.0	568.0	208.0	96.0	0.0	444.0	1165.0
Final Simulation	2734.7	2569.0	2435.3	1076.6	235.7	185.2	0.0	0.0	275.9	1120.3
Design Phase	2598.1	2106.7	1084.4	370.2	0.0	0.0	0.0	0.0	0.0	520.9

Figure 39: Comparison of the monthly heating demand between Final Simulation, Monitoring and simulation results of variation with semi-synthetically generated weather file.

The monthly absolute and relative error between the simulation results of the scenario with semi-synthetically generated *weather file* with the *Monitoring, Final Simulation* and *Design Phase* are depicted in *Figure 40* and *Figure 41*.

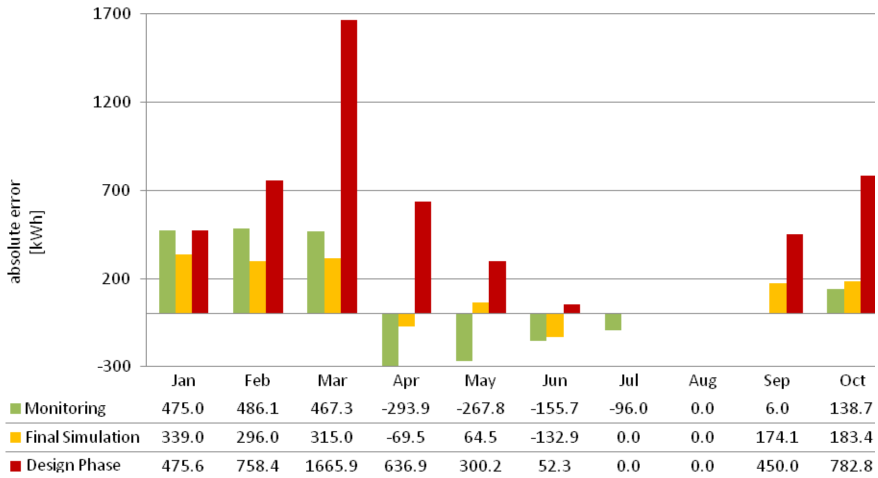

Figure 40: Monthly heating demand absolute error of the simulation with semi-synthetically generated weather data with Monitoring, Final Simulation and Design Phase.

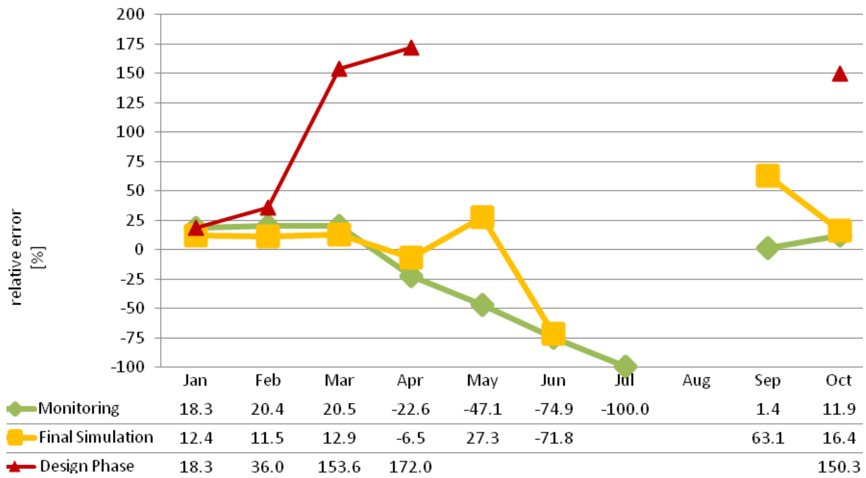

Figure 41: Monthly heating demand relative error of simulation results of variation with semi-synthetically generated weather file with Monitoring, Final Simulation and Design Phase

Heating

In the *Design Phase*, the heat set point was set according to Austrian standards to 20°C. However, the occupants adjusted the indoor air temperatures according to their comfort level; therefore the set temperatures were higher as assumed during this phase.

The results of the comparison of the simulation with set point temperature up to 20°C (*Ver2*) and the *Monitoring* showed that the heating energy consumption values predicted by *Ver2* were consistently lower. No heating energy demands were observed in May, June, July and September. The tendency of the comparison of *Ver2* with the actual users' set temperature profiles defined in the *Final Simulation* follows the previously described trend.

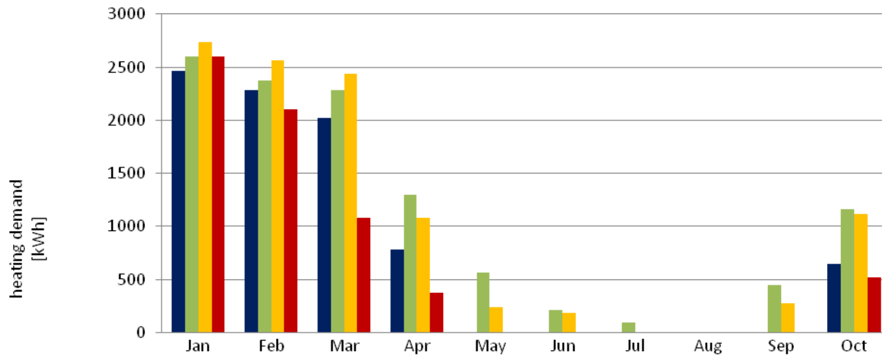

	Jan	Feb	Mar	Apr	May	Jun	Jul	Aug	Sep	Oct
Temperature-20°	2461.1	2283.9	2024.5	780.4	0.0	0.0	0.0	0.0	0.0	644.9
Monitoring	2598.7	2379.0	2283.0	1301.0	568.0	208.0	96.0	0.0	444.0	1165.0
Final Simulation	2734.7	2569.0	2435.3	1076.6	235.7	185.2	0.0	0.0	275.9	1120.3
Design Phase	2598.1	2106.7	1084.4	370.2	0.0	0.0	0.0	0.0	0.0	520.9

Figure 42: Comparison of the monthly heating demand between Final Simulation, Monitoring and simulation results of the version with the temperature set to 20°C.

The monthly absolute and relative error between the simulation results of the scenario with the temperature set to the constant value of 20°*C* with the *Monitoring*, *Final Simulation* and *Design Phase* are depicted in *Figure 43* and *Figure 44*.

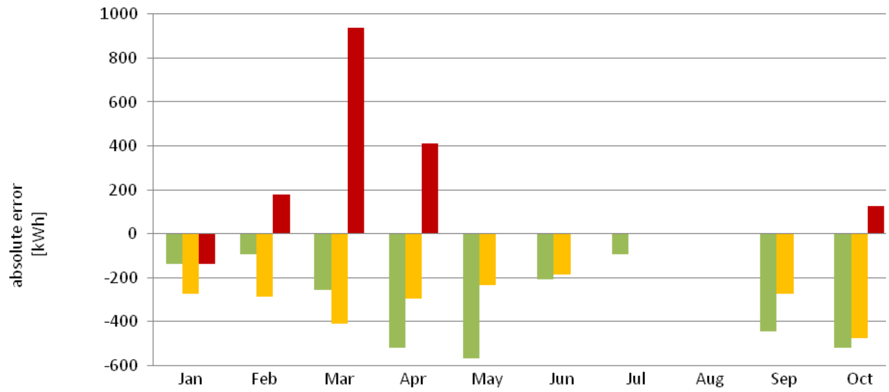

	Jan	Feb	Mar	Apr	May	Jun	Jul	Aug	Sep	Oct
Monitoring	-137.6	-95.1	-258.5	-520.6	-568.0	-208.0	-96.0	0.0	-444.0	-520.1
Final Simulation	-273.6	-285.1	-410.8	-296.3	-235.7	-185.2	0.0	0.0	-275.9	-475.4
Design Phase	-137.0	177.2	940.0	410.2	0.0	0.0	0.0	0.0	0.0	124.0

Figure 43: Monthly heating demand absolute error of simulation results of the Ver2 with Monitoring, Final Simulation and Design Phase

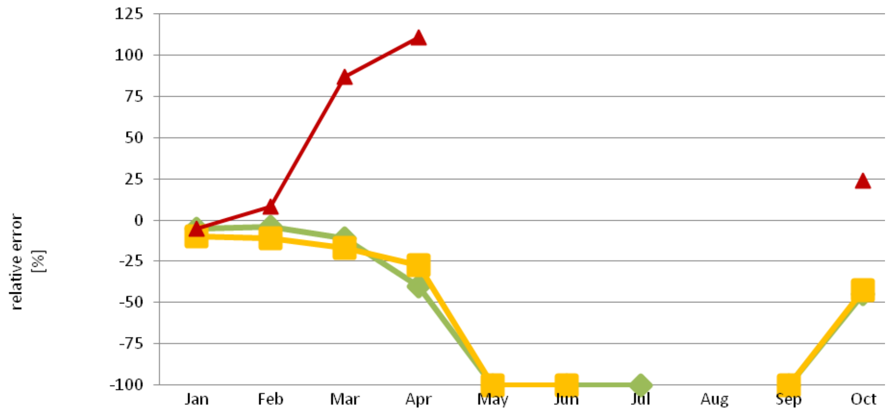

	Jan	Feb	Mar	Apr	May	Jun	Jul	Aug	Sep	Oct
Monitoring	-5.3	-4.0	-11.3	-40.0	-100.0	-100.0	-100.0		-100.0	-44.6
Final Simulation	-10.0	-11.1	-16.9	-27.5	-100.0	-100.0			-100.0	-42.4
Design Phase	-5.3	8.4	86.7	110.8						23.8

Figure 44: Monthly heating demand relative error of simulation results of the version with the temperature set to 20°C with Monitoring, Final Simulation and Design Phase.

Infiltration

In the *Ver3* model no infiltration rate was defined. The results of the comparison of *Ver3* with the *Monitoring* showed that the heating energy consumption values predicted by *Ver3* were consistently higher in January, February and March than the *Monitoring* in terms of the heating energy consumption. We can also observe underestimation of the heating demand in the warmer months April, May, June, July, September and October (cf. *Figure 45*).

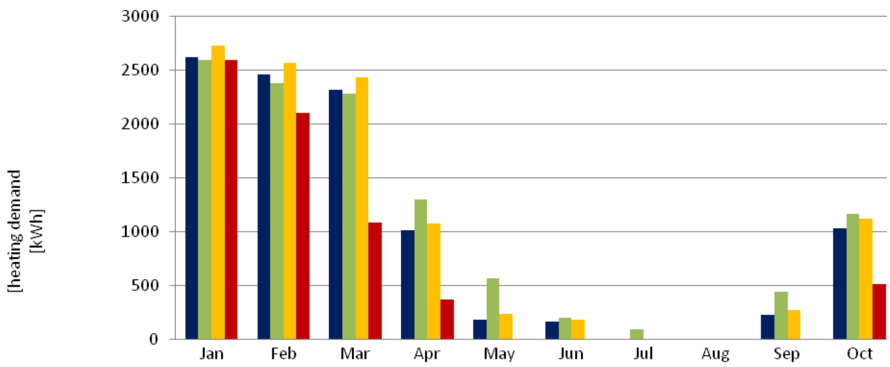

	Jan	Feb	Mar	Apr	May	Jun	Jul	Aug	Sep	Oct
No Infiltration Rate	2620.6	2466.9	2324.6	1013.6	190.9	167.7	0.0	0.0	230.8	1037.5
Monitoring	2598.7	2379.0	2283.0	1301.0	568.0	208.0	96.0	0.0	444.0	1165.0
Final Simulation	2734.7	2569.0	2435.3	1076.6	235.7	185.2	0.0	0.0	275.9	1120.3
Design Phase	2598.1	2106.7	1084.4	370.2	0.0	0.0	0.0	0.0	0.0	520.9

Figure 45: Comparison of the monthly heating demand between Final Simulation, Monitoring and simulation results of variation without defined infiltration rate.

The monthly absolute and relative error between the simulation results of the scenario with no infiltration rate defined with the *Monitoring*, *Final Simulation* and *Design Phase* are depicted in *Figure 46* and *Figure 47*.

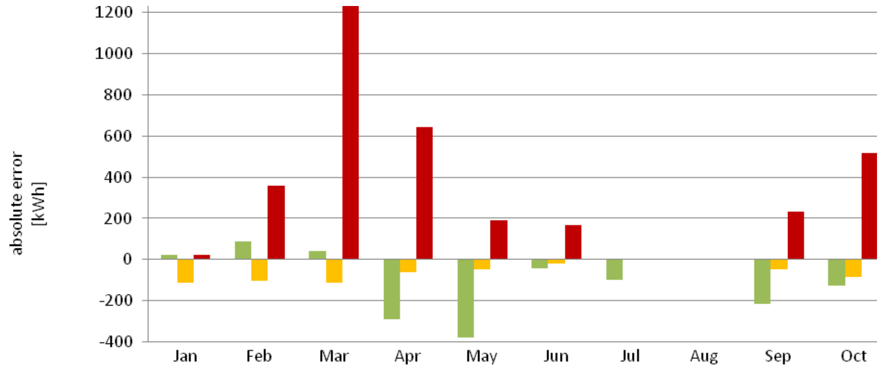

	Jan	Feb	Mar	Apr	May	Jun	Jul	Aug	Sep	Oct
Monitoring	21.9	87.9	41.6	-287.4	-377.1	-40.3	-96.0	0.0	-213.2	-127.5
Final Simulation	-114.1	-102.2	-110.7	-63.1	-44.8	-17.5	0.0	0.0	-45.1	-82.8
Design Phase	22.5	360.1	1240.1	643.3	190.9	167.7	0.0	0.0	230.8	516.6

Figure 46: Monthly heating demand absolute error of simulation results of variation without defined infiltration rate with Monitoring, Final Simulation and Design Phase.

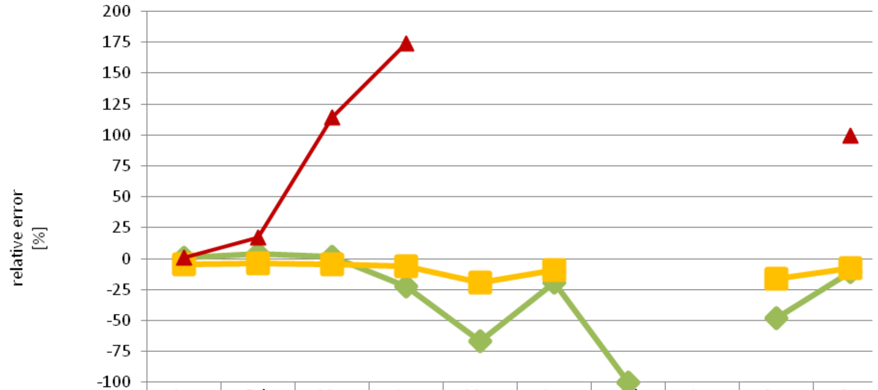

	Jan	Feb	Mar	Apr	May	Jun	Jul	Aug	Sep	Oct
Monitoring	0.8	3.7	1.8	-22.1	-66.4	-19.4	-100.0		-48.0	-10.9
Final Simulation	-4.2	-4.0	-4.5	-5.9	-19.0	-9.4			-16.3	-7.4
Design Phase	0.9	17.1	114.4	173.8						99.2

Figure 47: Monthly heating demand relative error of simulation results of variation without defined infiltration rate with Monitoring, Final Simulation and Design Phase.

Internal Gains

Internal heat gains are very often neglected when discussing effective energy. By internal gains we understand users' occupancy profiles as well as lighting profiles. However, it should be mentioned that light and other electrical equipment while being switched on, or additional people entering the building raise the temperature inside and reduce the heating demands at the same time.

The model *Ver4* presents a simulation scenario where internal gains were not defined at all.

The comparison between *Ver4* and *Monitoring* shows that the heating energy consumption predicted by V*er4* is consistently higher during the majority of the months than the monitored values (cf. *Figure 48*).

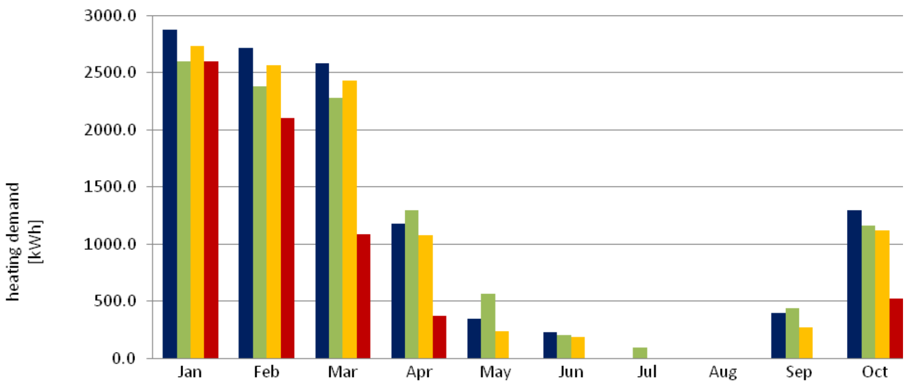

	Jan	Feb	Mar	Apr	May	Jun	Jul	Aug	Sep	Oct
No Internal Gains	2877.3	2715.2	2580.9	1179.5	351.9	228.5	0.0	0.0	394.9	1296.6
Monitoring	2598.7	2379.0	2283.0	1301.0	568.0	208.0	96.0	0.0	444.0	1165.0
Final Simulation	2734.7	2569.0	2435.3	1076.6	235.7	185.2	0.0	0.0	275.9	1120.3
Design Phase	2598.1	2106.7	1084.4	370.2	0.0	0.0	0.0	0.0	0.0	520.9

Figure 48: Comparison of the monthly heating demand between Final Simulation, Monitoring and simulation results of variation without defined internal gains.

The monthly absolute and relative error between the simulation results of the scenario with no internal gains with the *Monitoring*, *Final Simulation* and *Design Phase* are depicted in *Figure 49* and *Figure 50*.

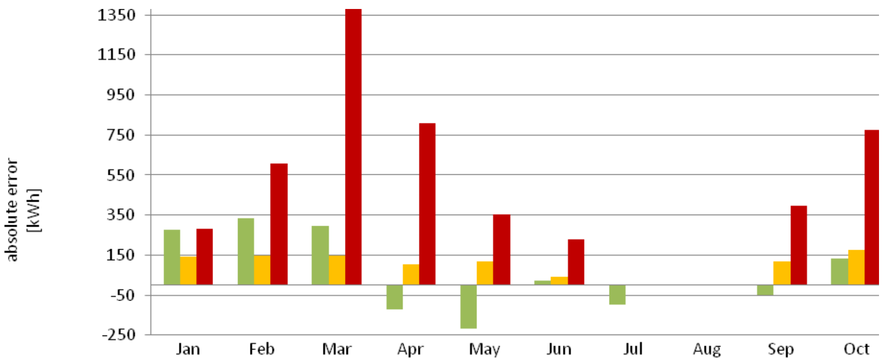

	Jan	Feb	Mar	Apr	May	Jun	Jul	Aug	Sep	Oct
Monitoring	278.6	336.2	297.9	-121.5	-216.1	20.5	-96.0	0.0	-49.1	131.6
Final Simulation	142.5	146.2	145.6	102.9	116.1	43.3	0.0	0.0	119.0	176.3
Design Phase	279.2	608.5	1496.5	809.3	351.9	228.5	0.0	0.0	394.9	775.7

Figure 49: Monthly heating demand absolute error of simulation results of version without defined internal gains with Monitoring, Final Simulation and Design Phase.

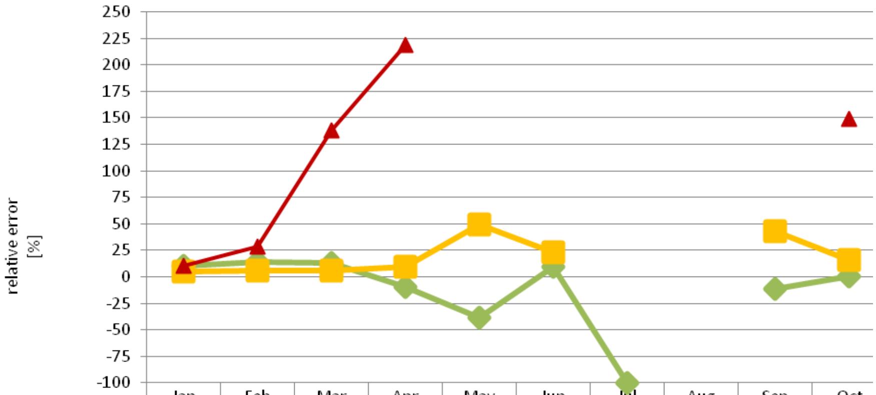

	Jan	Feb	Mar	Apr	May	Jun	Jul	Aug	Sep	Oct
Monitoring	10.7	14.1	13.0	-9.3	-38.0	9.8	-100.0		-11.1	0.1
Final Simulation	5.2	5.7	6.0	9.6	49.3	23.4			43.1	15.7
Design Phase	10.7	28.9	138.0	218.6						148.9

Figure 50: Monthly heating demand relative error of simulation results of version without defined Internal Gains with Monitoring, Final Simulation and Design Phase.

Ventilation

In the *Design Phase* model, the ventilation was defined as a constant exchange rate of the air equal to 0.17 ACH. However, the actual ventilation in the building is realized due to hygienic needs by window venting. This is taken into account in the final model, where the different ventilation rates for each zone based on the ASHRAE Standard 62-2001 and the CO_2 decay curve were defined. The comparison of the simulation with a constant air change rate of 0.17 ACH and the *Monitoring* showed that the monitored heating energy consumption values were consistently higher than the results of *Ver5*. We can also observe underestimation of the heating demand in the comparison with the *Final Simulation* over the entire analyzed period (cf. *Figure 51*).

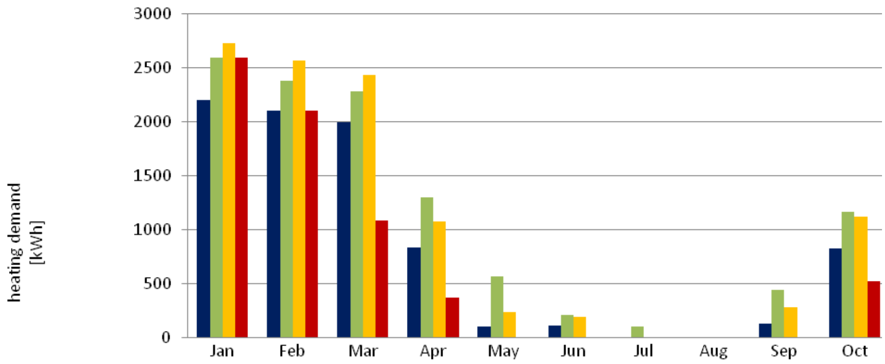

	Jan	Feb	Mar	Apr	May	Jun	Jul	Aug	Sep	Oct
Ventilation- 0.17 ACH	2203.7	2101.0	1992.9	831.6	97.8	111.2	0.0	0.0	122.3	829.2
Monitoring	2598.7	2379.0	2283.0	1301.0	568.0	208.0	96.0	0.0	444.0	1165.0
Final Simulation	2734.7	2569.0	2435.3	1076.6	235.7	185.2	0.0	0.0	275.9	1120.3
Design Phase	2598.1	2106.7	1084.4	370.2	0.0	0.0	0.0	0.0	0.0	520.9

Figure 51: Comparison of the monthly heating demand between Ver5, Monitoring, Final Simulation and Design Phase.

The monthly absolute and relative error between the simulation results of the scenario with the ventilation set to the constant value of 0.17 ACH with the *Monitoring*, *Final Simulation* and *Design Phase* are depicted in *Figure 52* and *Figure 53*.

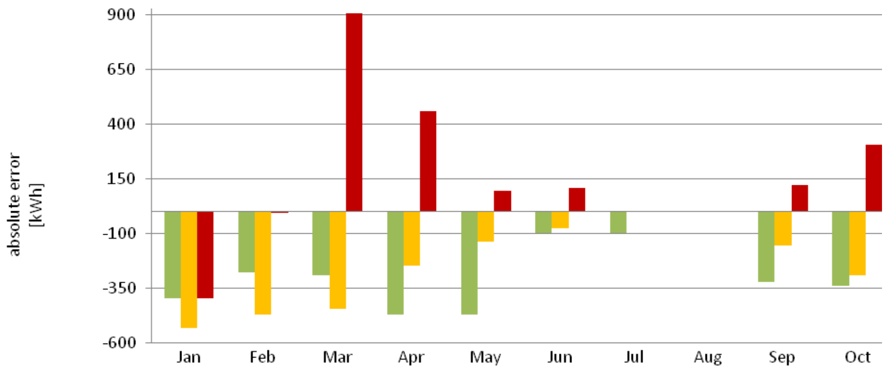

	Jan	Feb	Mar	Apr	May	Jun	Jul	Aug	Sep	Oct
Monitoring	-395.0	-278.0	-290.1	-469.4	-470.2	-96.8	-96.0	0.0	-321.7	-335.8
Final Simulation	-531.1	-468.0	-442.3	-245.1	-138.0	-74.0	0.0	0.0	-153.6	-291.1
Design Phase	-394.4	-5.7	908.5	461.3	97.8	111.2	0.0	0.0	122.3	308.3

Figure 52: Monthly heating demand absolute error of simulation results of variation with ventilation value set to 0.17 ACH with Monitoring, Final Simulation and Design Phase.

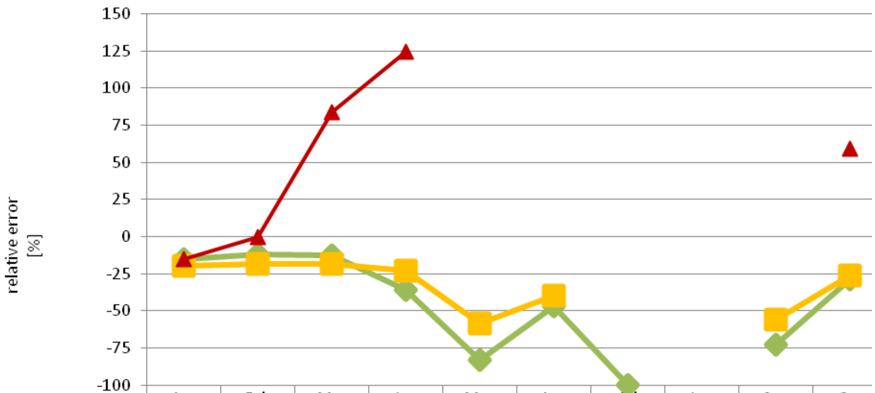

	Jan	Feb	Mar	Apr	May	Jun	Jul	Aug	Sep	Oct
Monitoring	-15.2	-11.7	-12.7	-36.1	-82.8	-46.6	-100.0		-72.4	-28.8
Final Simulation	-19.4	-18.2	-18.2	-22.8	-58.5	-40.0			-55.7	-26.0
Design Phase	-15.2	-0.3	83.8	124.6						59.2

Figure 53: Monthly heating demand relative error of simulation results of variation with ventilation value set to 0.17 ACH with Monitoring, Final Simulation and Design Phase.

Summary

After analyzing the factors influencing the heating demand of the different versions of the model, we observed significant impacts of the particular factors on the simulation performance. This analysis was carried out on a monthly basis. *Table 16* summarizes the evaluated versions and gives the accuracy of the simulation results in the monthly performance. None of the simulation versions registered a heating demand in July and August. The *Monitoring* data is regarded as 100% accurate by definition.

	Jan	**Feb**	**Mar**	**Apr**	**May**	**Jun**	**Sep**	**Oct**
Monitoring	100	100	100	100	100	100	100	100
Design	0	-11.4	-52.5	-71.5	-100	-100	-100	-55.3
Version 1*	+18.3	+20.4	+20.5	-22.6	-47.1	-74.9	+1.4	+11.9
Version 2*	-5.3	-4.0	-11.3	-40.0	-100	-100	-100	-44.6
Version 3*	+0.8	+3.7	+1.8	-22.1	-66.4	-19.4	-48.0	-10.9
Version 4*	+10.7	+14.1	+13.0	-9.3	-38.0	+9.8	-11.1	+11.3
Version 5*	-15.2	-11.7	-12.7	-36.1	-82.8	-46.6	-72.4	-28.8
Final Model	+5.2	+8.0	+6.7	-17.2	-58.5	-11.0	-37.9	-3.8

* *Version 1*: semi-synthetically generated weather file; *Version 2*: set heating point 20°C; *Version 3*: no infiltration rate; *Version 4*: no internal gains; *Version 5*: *ventilation value set to 0.17 ACH.*

Table 16*: Accuracy of the simulated models in percent.*

Figure 54 shows the total heating energy demand over the entire year. The monitored heat delivered is 11042.7 kWh, and the result of the closest matching simulation model (*Final Model*) is 10632.9 kWh.

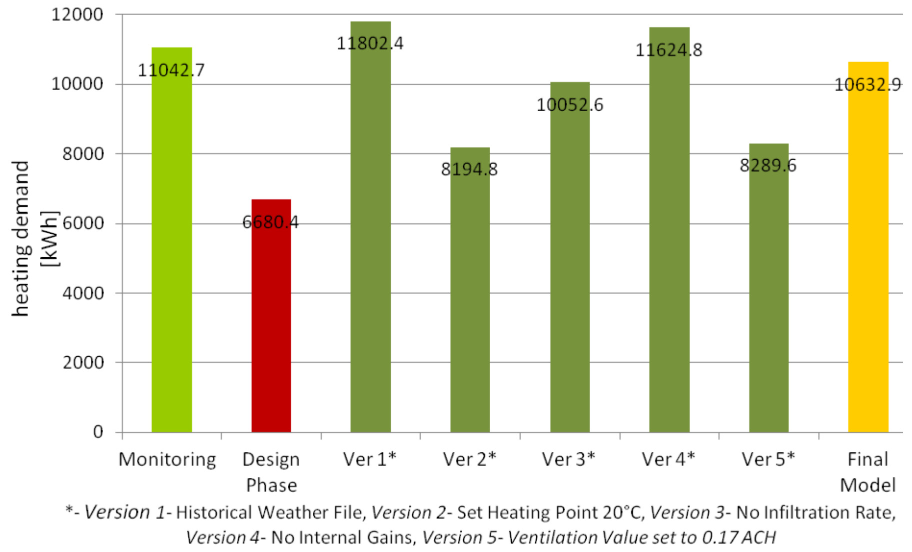

Figure 54: Comparison of the heating energy demand in the monitored period.

The annual absolute and relative error between the simulation results of different scenarios (including *Design Phase*) with the *Monitoring* are depicted in Figure 55 and Figure 56. These charts show the dramatic underestimation during the initial building design. As expected, the final simulation model provides the most accurate data.

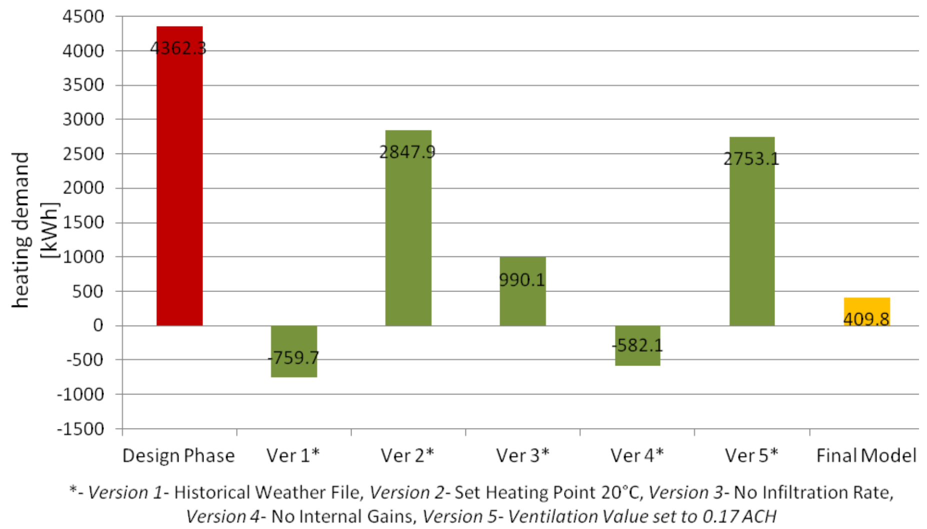

Figure 55: Absolute error of the heating energy demand compared to the Monitoring.

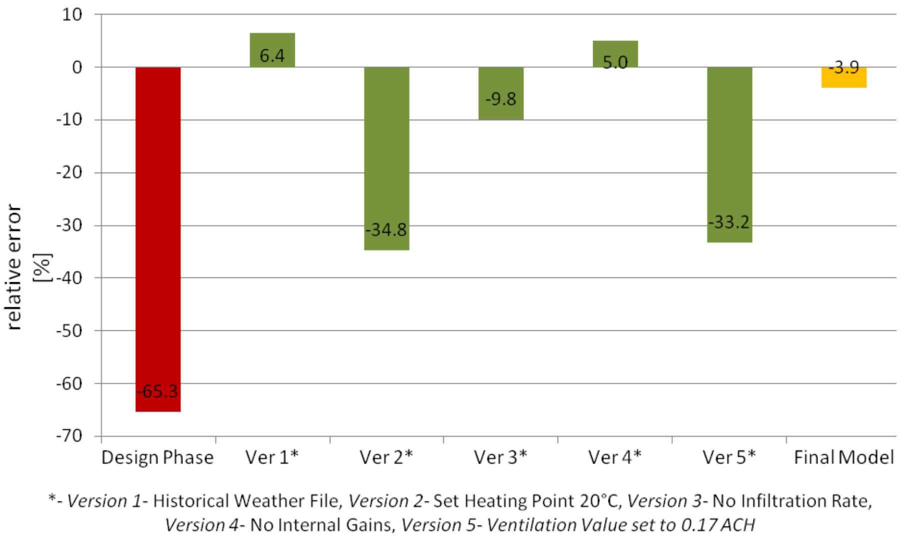

Figure 56: Relative error of the heating energy demand compared to the Monitoring.

7 CONCLUSION

After comparing the calibrated simulation (*Final Model*) with the monitored performance in terms of the heating demand, the annual relative error of the model was -3.9% and the absolute error was 409.8 kWh. The heating demand is higher than the monitored values during the winter months and lower in the summer time, when the heating demand was low in general.

The factors influencing the heating energy demand of the simulation in comparison to the *Monitoring* are the heating set points (-34.8% difference of the annual value), ventilation variation (-33.2%), infiltration rate (-9.8%), the weather file (6.4%) and internal gains (5%).

For the future work it is recommended to take deeper look into heating system efficiency, thermal heat losses of the water storage, external shades and night ventilation. These are also known to influence the thermal simulation results, however are not in the scope of this thesis due to the unavailability of their monitored data.

Our proposed model for generation of input data and its consistency of representing actual phenomena shows a potential of applying similar techniques. The introduced method can help understanding the calibration processes of the building model with on-site monitoring systems in further research.

Literature

Andrews, C.J., H. Chandra Putra, and C. Brennan. 2013. *Simulation Modeling of Occupant Behavior in Commercial Buildings*. Prepared by the Center for Green Building at Rutgers University for the Energy Efficient Buildings Hub, Philadelphia, PA.

ANSI/ASHRAE Standard 55-2013, *Thermal Environmental Conditions for Human Occupancy*.

Baker, N., 2013. *Natural ventilation: stack ventilation*. Research Associate, The Martin Centre, University of Cambridge. Internet. Available from http://www.architecture.com/RIBA/Aboutus/SustainabilityHub/Designstrategies/Air/1-2-1-2-Naturalventilation-stackventilation.aspx; accessed 15 May 2014.

Bekö, G., Gustavsen, S., Frederiksen, M., Kolarik, B., Toftum, J. and Clausen, G. 2011. *Comparison Of Air Change Rates Obtained By Different Ventilation Measurement Techniques In Five Danish Homes*. Proceedings from Indoor Air 2011. no. 602.

Brandemuehl, M.J. and K.M. Field. 2011. *Effects of variations of occupant behavior on residential building net zero energy performance*. Proceedings of Building Simulation .: 12th Conference of International Building Performance Simulation Association, Sydney, 14-16 November 2011, pp. 2603-2610.

Bromley, M., 2008. *Understanding Heating and Cooling Degree Days*. BizEE Software. Degree Days.net. Internet. Available from http://www.degreedays.net/; accessed 10 April 2014

Disch, R. 2009. *The plusenergyhouse for every community*. Internet. Available from http://www.rolfdisch.de/files/pdf/BROSCHUERE_PLUSENERGIEHAUS_IN_JEDE_GEMEINDE_2_ENGLISCH.pdf; accessed 06 June 2014.

Duffy, M. J. (2013). A *TRaNsient SYstems Simulation Program*. Internet. Available from http://sel.me.wisc.edu/trnsys/index.html; accessed 15 May 2014

Joechl, P. 2013. *Performance of a Brick Made Solar Plus Energy Building* *and Assessment of its Modeling*. Master Thesis, Fachhochschule Technikum Wien.

Laussmann, D., and Helm, D. 2011. *Air Change Measurements Using Tracer Gases: Methods and Results. Significance of air change for indoor air quality, Chemistry, Emission Control, Radioactive Pollution and Indoor Air Quality*. Dr. Nicolas Mazzeo (Ed.), ISBN: 978-953-307-316-3, InTech, DOI: 10.5772/18600.

Sartori, I., Marszal, A., Napolitano, A., Pless, S., Torcellini, P. & Voss, K. (2010), *Criteria for Definition of Net Zero Energy Buildings*, EuroSun 2010, p. 25.

Selke, T., Stift, F., Lehmden, A. and Krel, K. (2012), *Zwischenbericht: Solares Plus Haus mit bauteilaktivierter Wärmespeicherung in Speicherziegeln - Teil I: Entwicklung des Gebäudes*, 52 References Project Report 1, AIT Austrian Institute of Technology GmbH Vienna/Austria, Vienna. FFG Project Code: 829719.

List of Tables

List of Figures

Appendix A – Tables

Short Name	Description	Unit	Min. Value	Max. Value	Avg. Value	SD (σ)
Indoor Climate						
IC-EGVor-T	first floor, entrance hall, room air temperature	°C	19.28	28.52	23.39	1.35
IC-OGGang-T	second floor, corridor, room air temperature	°C	21.47	29.01	24.16	1.32
IC-EGWohn-T	first floor, living room, room air temperature	°C	17.88	29.32	24.00	1.44
IC-EGWohn-RH	first floor, living room, humidity level	%	23.01	68.40	44.66	5.78
IC-EGWohn-CO2	first floor, living room, CO2 level	ppm	394	1146	625	92
IC-OGSchlaf-T	second floor, bedroom, room air temperature	°C	12.20	29.42	23.51	1.78
IC-OGSchlaf-RH	second floor, bedroom, humidity level	%	33.28	74.34	51.86	4.74
IC-OGSchlaf-CO2	second floor, bedroom, CO2 level	ppm	378	1995	756	209
IC-OGKind1-T	second floor, children room 1, room air temperature	°C	13.49	29.79	23.84	1.63
IC-OGKind1-RH	second floor, children room 1, humidity level	%	33.66	70.76	48.94	5.12
IC-OGKind1-CO2	second floor, children room 1, CO2 level	ppm	378	1519	658	129
IC-OGKind2-T	second floor, children room 2, room air temperature	°C	15.82	29.76	23.77	1.65
IC-OGKind2-RH	second floor, children room 2, humidity level	%	29.2	70.8	50.4	4.9
IC-OGKind2-CO2	second floor, children room 2, CO2 level	ppm	397	1527	745	151
IC-OGBad-T	second floor, bathroom, room air temperature	°C	18.07	29.80	24.80	1.39

Electrical Demand						
ED-Kueche-E	Electricity meter, Kitchen Block	kWh	153.7	810.6	518.9	190.2
ED-Wohn-E	Electricity meter, lighting kitchen / living room	kWh	71.3	211.5	159.8	33.6
ED-Gang-E	Electricity meter lighting corridor / Office	kWh	46.7	249.2	170.3	50.7
ED-Dach-E	Electricity meter second floor	kWh	148.8	320.8	235.4	44.9
Heat balance						
HS-Col-E	energy delivered by the solar collectors	kWh	1842	14152		
HS-Bio-E	energy delivered by the biomass boiler	kWh	0	2610		
HT-BW-E	energy delivered by the wall heating	kWh	1330.8	5324		
HT-Floor-E	energy delivered by the floor heating	kWh	3605.3	10620		
HS-Water-E	energy delivered by the domestic hot water	kWh	102	2641		
HS-Col-P	energy transferred back to the ambient (if negative)	kW	-16.5	30.6		
Tank Temperatures						
HS-Storage-Td	water tank temperature at the height of 64cm (12%)	°C	24.0	92.4	54.5	24.2
HS-Storage-Tcd	water tank temperature at the height of 168cm (31%)	°C	24.0	92.4	54.5	24.2
HS-Storage-Tc	water tank temperature at the height of 287cm (52%)	°C	25.3	89.4	59.5	22.5
HS-Storage-Tuc	water tank temperature at the height of 406cm (74%)	°C	24.9	91.1	62.3	20.4
HS-Storage-Tu	water tank temperature at the height of 482cm (88%)	°C	26.0	92.1	67.0	20.2
HS-Storage-Twater	water tank temperature at the height of 524cm (95%)	°C	34.6	92.1	74.2	10.4
Outdoor Climate (ZAMG - Zentralanstalt für Meteorologie und Geodynamik)						
FFX	ambient humidity level	%	34.4	99	84.2	15.4
GSX	global radiation	J/cm²	0	730.7	94.9	162.2
TTX	ambient temperature	°C	-16.3	34.9	7.5	8.5

Table 17: Documentation of the available data nodes.

Month	**Start Day**	**Start Hour**	**End Day**	**End Hour**	**Nr of days**
January	2013-01-01	1:00:00	2013-02-01	2:00:00	31
February	2013-02-01	2:00:00	2013-03-01	1:00:00	28
March	2013-03-01	1:00:00	2013-04-01	1:00:00	31
April	2013-04-01	1:00:00	2013-05-02	1:00:00	31
May	2013-05-02	1:00:00	2013-06-01	1:00:00	30
June	2013-06-01	1:00:00	2013-07-01	1:00:00	30
July	2013-07-01	1:00:00	2013-08-01	1:00:00	31
August	2013-08-01	1:00:00	2013-09-01	1:00:00	31
September	2013-09-01	1:00:00	2013-10-01	1:00:00	30
October	2013-10-01	1:00:00	2013-11-01	1:00:00	31
November	2013-11-01	1:00:00			

Table 18: Table with applied time periods, which are adapted to the available monitoring data.

Appendix B – Documents

Combined sensor CO2/ Temp./ relative Humidity – WRF04 CO2/ LK CO_2

The sensor is designed for the detection of carbon dioxide (CO2), temperature and relative humidity (optionally) in living spaces. Wherever people are staying in rooms, the CO2 concentration is an evident indicator for the room quality.

For the CO2 measurement the 'Non Dispersive InfraRed (NDIR) Technology' with automatic self-calibration is used. For a direct locking-on to a DDC or a monitoring system, analog 0...10V outputs are available. Additionally, the device is supplied with a passive temperature sensor.

Technical Details:

Room sensor for measuring the CO2 concentration and temperature in rooms

Measuring range 0...2000ppm and 0...50°C

Output 0...10V

Power supply 15-24DC/24VAC

Passive temperature sensor

Optionally with LCD display to show CO2 concentration, temperature and rel. humidity

Optionally with 3 LED to show the CO2 concentration

Optionally with analog output for relative humidity

Technical Data:

Power supply: 15-24VDC (±10%)

Power consumption: max. 3W

Analog outputs: CO2, 0…10V, load max. 10mA

Temp., 0...10V, load max 10mA

Rel. humidity, 0...10V, max. load 10mA

CO2 Sensor: 0...2000ppm, NDIR (non dispersive infrared)

Temp. Dependence: CO2: <0,2% of Full Scale per °C

Accuracy @21°C: CO_2: typ. ±40ppm + 4% of reading

Temp.: Typical ±1K of full scale

Humidity: Typ. ±3% (between 20... 80% rH)

Warm Up Time: < 2 minutes

Response Time: < 10 minutes

Stability CO_2: < 2% Full Scale over life of sensor (typ. lifetime 15 years)

Repeatability CO_2: <1% of Full Scale

(Source: AIT GmbH, 2014)

Electronic polyphase meter for Smart Metering and other sophisticated applications - AS1440

The AS1440 meets the conditions for precise measurement, safe storage and reliable data transfer. The meter is available for either direct or CT/VT connections. Measurements can be done for all four quadrants. In addition the AS1440 can be equipped with anti-tampering features resp. the detection of manipulation attempts. For remote readings communication modules for WAN-comm. are available (e.g. GSM/GPRS, PLC), as well as M-BUS module for HAN-comm. to gas or water meters.

Furthermore a connect/disconnect relay can be installed to switch of the consumer totally or at a parametrisible threshold.

Technical Data:

Nominal voltage: 4-wire, 3-systems, 3x220/380V .. 3x240/415V, -20% .. 15%

Nominal frequency: 50 / 60Hz, +/-5%

Nominal / maximum current: Continuous current- DC: 5(60)A, 5(80)A, 5(100)A, 5(120)A, CT: 5//1, 1(2)A, 5(6)A, 5(15)A, …

Short duration- DC: 7000A for 2 cycles,

CT: 300A for 0,5s

Starting current: DC / CT- 20mA / 1mA

Power supply: Nominal voltage- Still operates even with the failure of two phases or one phase and the neutral

(Source: AIT GmbH, 2014)

Room Sensor Wall Mounted - WRF04 TRV

The room operating panel is designed for temperature detection

Technical Data:

Power supply: TRV: 15-24V= (10%) or 24V (10%)

Power consumption: TRV: max. 12mA/24V

Measuring range: adjustable at the transducer

Output: 0...10V, min. load 5kΩ

Accuracy@21°C: ± 1% of full scale

(Source: AIT GmbH, 2014)

Table 19: *Sensors and instruments specification inside of the building*

Gealog NTC Air Temperature Sensor	Technical Data:
Air temperature sensor based on a high precision NTC-Thermistor net-	Measuring range -50°C to +60°C Uncertainty: 0,1K

work.  *(Source: Logotronic)*	Response time T66 < 10 s
Starpyranometer – Schenk, Type 8101	Technical Data:
The Starpyranometer is used for measuring global and reflected global radiation and solar radiation on surfaces inclined to the horizontal.  *(Source: Schenk)*	Measuring range: 0 ... 1500 Wm-2 Spectral sensivity: 0.3 ... 3 µm Output: appr. 15 µV/Wm-2 lmpedance: appr. 35 Ohm Ambient temperature: - 40°C ... + 60°C

Table 20: Sensors and instruments specification of the ZAMG weather station.